
Scientific Language Modeling: A Quantitative Review of Large Language Models in Molecular Science

Pengfei Liu

Peng Cheng Laboratory
School of Computer Science and Engineering,
Sun Yat-sen University

Jun Tao

School of Computer Science and Engineering,
Sun Yat-sen University

Zhixiang Ren*

Peng Cheng Laboratory
renzhx@pcl.ac.cn

ABSTRACT

Efficient molecular modeling and design are crucial for the discovery and exploration of novel molecules, and the incorporation of deep learning methods has revolutionized this field. In particular, large language models (LLMs) offer a fresh approach to tackle scientific problems from a natural language processing (NLP) perspective, introducing a research paradigm called scientific language modeling (SLM). However, two key issues remain: how to quantify the match between model and data modalities and how to identify the knowledge-learning preferences of models. To address these challenges, we propose a multi-modal benchmark, named ChEBI-20-MM, and perform 1263 experiments to assess the model's compatibility with data modalities and knowledge acquisition. Through the modal transition probability matrix, we provide insights into the most suitable modalities for tasks. Furthermore, we introduce a statistically interpretable approach to discover context-specific knowledge mapping by localized feature filtering. Our pioneering analysis offers an exploration of the learning mechanism and paves the way for advancing SLM in molecular science.

Keywords Large Language Model · Molecular Science · Benchmarking

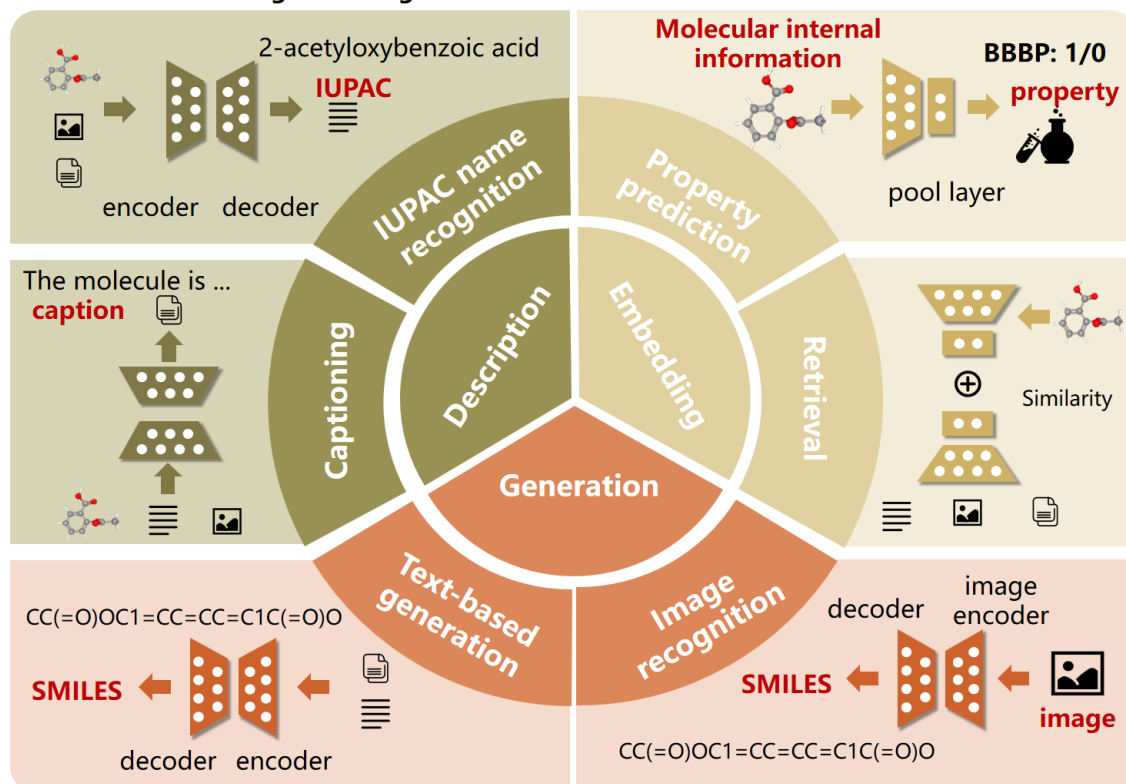
1 Introduction

Molecular modeling and design are pivotal in the discovery and development of new molecules, serving a wide range of applications from drug discovery to materials science. Nevertheless, traditional approaches to discovering new molecules or refining existing ones are often arduous, costly, and fraught with a high risk of failure. In contrast, modern computational approaches significantly improve the creation and modification of molecules. These techniques speed up the identification and optimization of drug candidates, enhancing discovery efficiency. Yet, they require considerable computational resources. Artificial Intelligence (AI) methods have made significant strides in this domain. They offer faster computations and the ability to handle large datasets. Various machine learning [1] and graph models [2] [3] [4] are employed for molecular property prediction, while generative models [5] [6] [7] are utilized for molecular design. However, most AI models often face challenges in generalizability and flexibility, requiring extensive data for training to ensure accuracy and require specific adjustments for each molecular task.

Transformers [8] offer an advantage with their robust text encoding and generation capabilities. These models can be fine-tuned with minimal task-specific adjustments, making them more versatile and efficient in molecular modeling and design. Moreover, since the advent of ChatGPT [9] and GPT-4 [10], LLMs have emerged as a groundbreaking trend, especially in molecular science. LLMs, with their advanced capabilities in processing and generating human-like text, present a novel paradigm for understanding and designing molecular structures. Their ability to assimilate and analyze vast amounts of textual data can provide unprecedented insights, overcoming some of the limitations of traditional AI

*Corresponding author

a. Molecular modeling and design tasks



b. The processes of tasks

		Tasks with Their Inputs and Outputs							
		graph	SMILES	InChI	SELFIES	caption	IUPAC	property	image
Internal information	graph		⑦	⑦	⑦	① ④	② ④	③	⑦
	SMILES	⑦		⑦	⑦	① ④	② ④	③	⑦
	InChI	⑦	⑦		⑦	① ④	② ④	③	⑦
	SELFIES	⑦	⑦	⑦		① ④	② ④	③	⑦
External information	caption	⑨	⑤	⑨	⑨		②	⑧	⑨
	IUPAC	⑨	⑤	⑨	⑨	① ④		⑧	⑨
	property	⑨	⑨	⑨	⑨	⑨	⑨		⑨
	image	⑨	④ ⑥	⑨	⑨	① ④	② ④	⑧	

- ① Molecule captioning ④ Molecular retrieval ⑦ Tasks achievable through tools
 ② IUPAC name recognition ⑤ Molecule generation ⑧ Limitations due to data availability
 ③ Property prediction ⑥ Image recognition ⑨ Tasks beyond our scope

Figure 1: **The paradigm of the review.** a. **Molecular modeling and design tasks**, showcasing six task types with their standard modeling methods and data examples. b. **The processes of tasks**, we divide common molecular data into two categories: internal and external information. Internal information, integral to molecular representation, can be converted through various tools. External information is more accessible to human understanding. Additionally, this part highlights the research scope of our review, detailing the input and output for each task.

methods. This new capability combines accuracy and novelty for improved outcomes, termed chemical knowledge. Its

effectiveness depends on factors like input data, model architecture, and training strategies. However, current reviews and benchmark assessments of this capability are not comprehensive.

Existing surveys in molecular science, like the molecule-generation survey [11], often lack comprehensive model comparisons and have a limited task scope. The knowledge-driven survey [12] categorizes molecular learning but misses detailed method comparisons and dataset discussions. And recent benchmarks, such as one testing ChatGPT [13], cover eight chemical tasks, each providing unique chemical insights. Mol-Instructions [14] offers a dataset for fine-tuning with various molecule and protein instructions, boosting biomolecular understanding in LLMs. However, these surveys and benchmarks lack multi-modal content and do not sufficiently explore the models’ chemical knowledge.

In summary, this study comprehensively reviews Transformers and LLMs in molecular modeling and design. We categorize six common molecular tasks into three distinct objectives: description, embedding, and generation, as vividly depicted in Figure 1. Moreover, we establish a unified multi-modal benchmark ChEBI-20-MM and conduct experiments to assess the compatibility of data modalities, model architectures, and diverse task types, examining their impact on task performance. Additionally, our end-to-end visual method showcases the discovery of modeling insights embedded with chemical knowledge. Overall, our main contributions are the following:

- This work analyzes LLMs in molecule modeling, categorizes existing models, and presents a multi-modal benchmark (ChEBI-20-MM) for performance evaluation, backed by **1263** experiments.
- We analyze the modal transition probability matrix and identify **best match** between different data modalities and model architectures.
- We introduce a statistically interpretable approach to showcase the **knowledge acquisition** through localized feature filtering.

The rest of this paper is organized as follows. Section 2 introduces relevant definitions and background. Then, we explore six critical tasks in molecular modeling and design. Section 3 presents our benchmark and insights. Section 4 discusses key results and limitations, and Section 5 concludes with a summary of our contributions and future research directions.

2 Methodology

In this section, we present essential background information. We start by defining different molecular representation forms and vital data sources, then move to discuss LLMs, highlighting their significance in this field.

2.1 Molecular Representation

Molecular structures can be represented in multiple ways for computational analyses, each with advantages and limitations. These include graph structures, images, as well as one-dimensional notations. Figure 1. a showcases examples of various data representation forms, while Figure 1. b categorizes these representations into molecular internal and external information. Additionally, it illustrates the relationships between these forms of representation and their corresponding tasks.

In terms of molecular internal information, **SMILES** (Simplified Molecular Input Line Entry System) [15] offers a widely-used one-dimensional notation for describing molecular structures. **InChI** (International Chemical Identifier) [16] provides a unique identifier for chemical substances, facilitating the standard encoding of molecular information. Further advancing molecular representations, **SELFIES** (Self-Referencing Embedded Strings) [17] offers machine learning-oriented approaches, addressing the limitations of SMILES. Moreover, graph structures naturally represent molecules, with atoms as nodes and bonds as edges, effectively capturing both local and global topological traits.

For external molecular information, **images** offer a visual 2D or 3D representation of molecules. **IUPAC** (International Union of Pure and Applied Chemistry) [18] names provide a standardized naming system for organic compounds. Additionally, molecular **properties** serve as a form of representation aiding human comprehension. Furthermore, the molecular **captions** offer rich contextual information, encompassing textual descriptions of functions, properties, and inter-molecular relationships.

2.2 The Databases and Datasets for Molecular Science

In this section, we highlight vital data sources essential for molecular science research. As detailed in Table 1, PubChem and ZINC databases provide extensive compounds for virtual screening. ChEMBL offers comprehensive data on bioactive molecules, while ChEBI focuses on cataloging small chemical compounds. DrugBank serves as a valuable

resource for drug and target information. Lastly, the USPTO database, encompassing patent filings and research data, forms a vital part of the scientific literature.

Table 1: Overview of Data Sources for Molecular Science

Type	Data Source	Content	No. of Entries	Description
Database	PubChem [19]	compounds and substances	116M	molecule database
	ZINC [20]	compounds and substances	230M	virtual screening database
	ChEMBL [21]	compounds with text descriptions	2.4M	bioactive molecule database
	ChEBI [22]	small chemical compounds	61,032	molecular entity dictionary
	DrugBank [23]	small molecule drugs	12,695	drug/target database
	USPTO	patent filings and data	—	scientific corpus
Dataset	C4 [24]	Clean English text	—	Pretrain
	MoMu dataset [25]	Graph-document pairs	15,613	Pretrain
	MOSES [26]	Molecular structures	1.9M	Generation
	PCdes [27]	SMILES-text descriptions	1.5K	Molecular retrieval
	CheBI-20 [28]	SMILES-text descriptions	33,010	Generation and captioning
	PubChemSTM [29]	SMILES-text descriptions	281K	Generation
	Mol-Instructions [14]	SMILES-text descriptions	333K	Generation and captioning
	MoleculeNet [30]	Molecular properties.	700K	Property prediction
	USPTO(OSRA) [31]	Images and ground truth	5,719	Image recognition
	CLEF [32]	Images and ground truth	865	Image recognition
	JPO [31]	Images and ground truth	450	Image recognition
	UOB [33]	Images and ground truth	5,740	Image recognition
	USPTO-50k [34]	Chemical reactions	50K	Reactions prediction

Moreover, various vital datasets support a wide range of research, from pretraining to specific molecular science tasks. As shown in Table 1, the Colossal Clean Crawled Corpus (C4) dataset offers a vast amount of clean English text scraped from the web for the pretraining of the T5 model. MOSES provides molecular structures from ZINC, while MoleculeNet encompasses a broad spectrum of molecular property predictions ranging from quantum mechanics to biophysics and physiology. Additionally, datasets such as USPTO, CLEF, JPO, and UOB offer molecular images with ground truth, supporting image recognition tasks. The PCdes, CheBI-20, and PubChemSTM datasets, along with Mol-Instructions, provide essential SMILES-text pairs that facilitate cross-information retrieval, molecule generation, and molecular captioning tasks.

2.3 Large Language Models

Transformers, known for their self-attention mechanisms, enable the model to weigh the importance of different parts of the input data, which is crucial for understanding complex molecular structures of text modality. LLMs are Transformer-based models scaled to a large extent.

Among the notable backbone models in this domain are GPT [9] (Generative Pre-trained Transformer) and BERT [35] (Bidirectional Encoder Representations from Transformers). Especially in the fine-tuning stage, these models exhibit remarkable versatility and efficiency, requiring minimal task-specific adjustments for applications in molecular modeling.

- **Encoder-based models:** BERT and its derivatives like RoBERTa [36] and domain-specific variants such as SciBERT [37] and ChemBERTa [38] have been effectively employed for molecular property prediction.
- **Decoder-based models:** GPT-2 [9] and ChatGPT [39] are superior in text generation capabilities. Specific-domain models like MolXPT [40], based on GPT-2, and MolReGPT [41], based on ChatGPT, showcase strong performance in generating molecular sequences and descriptions.
- **Encoder-Decoder Models:** The Transformer architecture itself exemplifies an end-to-end model, with T5 [24] and BART [42] models further enhancing robust end-to-end text generation capabilities, advancing domain-specific applications. For instance, MolT5 [43] is tailored explicitly for molecule generation and description, while Text+Chem T5 [44] is adept at reaction prediction. Beyond these, Encoder-Decoder models also encompass multi-modal models. Prominent examples include BLIP2 [45] and Mini-GPT4 [46], based on large language model frameworks, and GIT-Mol [47], a multi-modal model capable of processing image, graph, and text data, demonstrating the versatility and adaptability of these models in handling diverse data types.

2.4 Language Modeling Tasks and Models in Molecular Science

In this section, we present a timeline showcasing the pivotal developments in transformer-based models for molecular modeling and design, alongside classifications and architectures, as illustrated in Figure 2. The Details of the models are shown in the Appendix. A Table 2.

Molecule captioning It aims to develop textual descriptions based on given molecular representations. It involves not only recognizing the molecular structure but also interpreting and conveying its functional properties, potential uses, and any relevant scientific context.

MolT5 [43] is a groundbreaking model that uses the T5 architecture for end-to-end text tasks, achieving exceptional performance in single-modality models. Following this, MolXPT [40], built on GPT-2, utilizes a large corpus of PubMed titles and abstracts along with SMILES sequences from PubChem [19]. It performs exceptionally well in few-shot learning and generative pre-training. As for multi-modality models, MoMu [25] and MolFM [64] employ cross-modal contrastive learning techniques. They fuse graphical and textual data through their encoders and use MolT5 as a decoder. MolCA [65] combines Q-Former with contrastive learning to integrate SMILES strings and graphs, leveraging Galactica’s [66] generative capabilities for captioning. In a similar vein, GIT-Mol [47] advances this integration with its more versatile GIT-Former architecture, processing text, graphs, and images.

IUPAC Name Recognition Unlike free-form textual descriptions, IUPAC names possess the advantage of uniformity and specificity, making them highly structured and predictable. Furthermore, the task of IUPAC name recognition involves not just the decoding of these structured names but also understanding the underlying molecular structure they represent. Struct2IUPAC [67] employs a Transformer-based architecture, complemented by a specialized tokenizer adept at processing both SMILES strings and IUPAC nomenclature. Moreover, the TransAntivirus [68] goes a step further by adopting the versatile T5 model architecture. This approach not only enables conversions but also facilitates the evaluation of generated molecules on multiple metrics, including uniqueness, validity, and a range of chemical properties.

Molecular Property Prediction Molecular representation is critical in molecular modeling, providing ways to describe and encode molecular structures for computational use. Within this domain, molecular property prediction is essential, assessing attributes like solubility, toxicity, and protein binding affinity. Based on BERT, KV-PLM [27] employs a dual tokenizer to better recognize specific atoms and functional groups within SMILES strings. LLM4Mol [69] leverages the power of LLMs to introduce a novel molecular representation through text-based explanations. As for multi-modal methods, MoMu [25] applies contrastive learning techniques to assimilate modality-specific and complementary information from text and graph data. Post-encoding, embeddings are transformed into fixed-length vectors via a pooling layer, employing methods like average pooling and max pooling. **Average pooling** calculates the mean of all sequence vectors for a general context representation. **Max pooling** selects each feature’s maximum value across the sequence, highlighting key molecular features.

Molecular Retrieval Molecular retrieval aims for efficient, accurate identification of molecules in large datasets. Its effectiveness relies on the type of molecular data used, like structural formulas or SMILES strings. In cross-modal retrieval tasks, Text2Mol [28] excels by combining natural language with molecular data into a unified semantic space for effective retrieval. Similarly, MoMu [25] and MolFM [64] use advanced contrastive learning to merge text and molecular graphics, enhancing the feature space for robust retrieval tasks. As for the pooling layers, similar to those detailed in the molecular property prediction section. This process ensures that the final vectors retain the most salient features from both textual and graphical inputs, enabling more accurate and efficient molecular retrieval.

Molecular Image Recognition In our research, molecular image recognition focuses on converting visual representations of molecular structures into standardized, textual formats like SMILES. This task is particularly crucial for automating the interpretation of chemical literature, where molecular images are frequently used to describe compounds. DECIMER 1.0 [70], Image2SMILES [71] and MICER [72] employ Transformer-based architectures and image augmentation, handling large datasets effectively. SwinOCSR [73] utilizes Swin Transformers [74] for global feature extraction and tackles token imbalance with focal loss, streamlining DeepSMILES generation. Additionally, MolScribe [75] shows strong performance against low-quality images and includes confidence assessment for its predictions, enhancing output reliability.

Molecule Generation Our research focuses on developing one-dimensional textual representations, particularly in SMILES format. This includes text-based de novo molecule generation and molecular optimization, due to their methodological similarities. In molecular generation, models adept at molecule captioning are equally capable of

Transformers with its efficiency. BioT5 [76] further expands this to include protein-related texts, focusing on SELFIES and extending to Protein Property Prediction and Drug-target Interaction.

Molecular optimization aims to refine molecules for improved properties, aligning with generative goals. MolGPT [77] utilizes the GPT architecture’s self-attention and conditional generation for effective molecule control and property-based generation. MoleculeSTM [29] employs MegaMolBART[78] and contrastive learning on graphs and text, optimizing target attributes like binding affinity and drug-relatedness with precision. ChatMol [79] takes an interactive approach, combining empirical data, spatial knowledge, and language associations for enhanced molecular design.

3 Evaluation and Results

In this chapter, we propose ChEBI-20-MM, a comprehensive benchmark developed from the ChEBI-20 dataset, integrating multi-modal data such as InChI, IUPAC, SELFIES, and images. This benchmark is designed to assess the chemical knowledge of models across tasks such as molecule generation, image and IUPAC recognition, molecular captioning, and retrieval, featuring in-depth analysis of the compatibility between modalities and models, as well as an exploration into models’ tendencies for knowledge acquisition.

3.1 ChEBI-20-MM and Experimental Setup

In molecular representations, molecular text descriptions, typically scarce, now see increased utilization with MolT5’s ChEBI-20 dataset in molecule generation and captioning. To facilitate multi-modal data evaluation, we expand our data modality variety, introducing ChEBI-20-MM. This benchmark effectively evaluates the versatility of data types and model combinations in describing, generating, and embedding molecular data. Figure 3 showcases our evaluation of prevalent backbone models and experiments. For comparing models’ embedding capabilities, our experiments include datasets from MoleculeNet, enabling thorough assessments in biochemical and physicochemical contexts.

We conduct 1263 experiments, encompassing 291 generative and retrieval tasks from the ChEBI-20-MM benchmark and 972 property prediction experiments. For text-to-text tasks, our models include 11 architectural variations, combining three decoder-only models, four encoder-decoder models, and four composite models with MolT5 as the decoder paired with various encoders. We conduct experiments based on the setup, performing each experiment three times to calculate the mean and standard deviation of the results. Then, we analyze the **suitability** of data sources for language models and **chemical space coverage**, as shown in Appendix. B Figure 6. The description of the metrics is also located in Appendix B.

3.2 Experimental Results

For the analysis of modality adaptation to different tasks, as depicted in Figure 4. a. We select representative metrics indicative of successful task completion, such as the METEOR score for molecule captioning and the ROC_AUC for property classification tasks. We fill out the modal transition probability matrix, which provides insights into the most suitable data modalities for different task types. Regarding model analysis for different tasks, Figure 4(b) and (c) demonstrate the frequency of appearances of encoders and decoders in nine text-to-text tasks, as well as eight encoders and two pooling mechanisms in embedding tasks. Detailed experimental results are shown in Appendix. C Table 3-Table 7. From the results, we present the following **modality insights**:

- **IUPAC Names for Generation and Captioning:** IUPAC names are conducive to text-based molecule generation and molecule captioning.
- **SMILES for IUPAC Recognition:** SMILES representations are particularly well-suited for IUPAC recognition compared to other molecular internal information.
- **Preferred Modalities for Captioning:** Since some captions include the IUPAC name of the molecule, IUPAC is the most appropriate modality for molecule captioning, followed by SMILES.
- **Choosing Modalities for Retrieval:** For molecule retrieval tasks targeting captions, IUPAC is the optimal modality, followed by SMILES. Conversely, when the target is IUPAC names, SMILES becomes the most favorable modality.
- **Graph vs. Textual Modalities in Property Prediction:** In molecular property prediction tasks, among the selected top five rank combinations from 90 groups, graph modalities appear 40 times and SMILES 25 times, indicating a clear advantage for graph modalities and the relative superiority of SMILES over other textual representations.

As for the **model performance insights**:

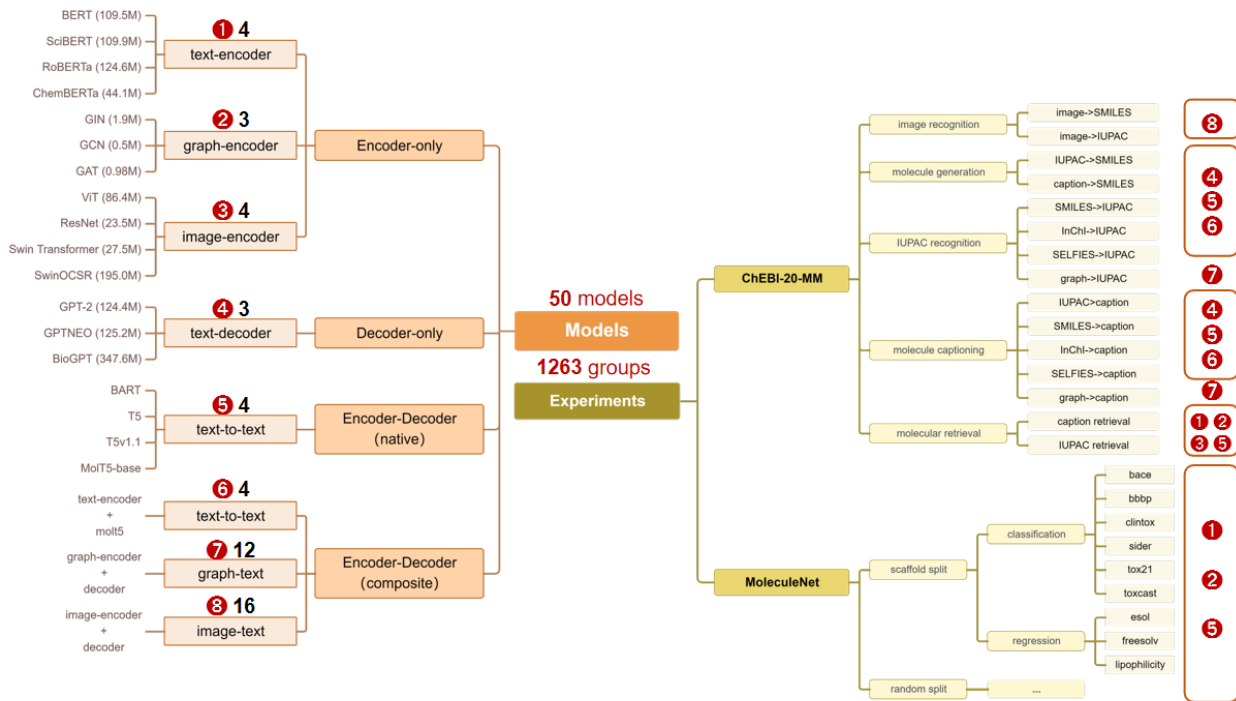


Figure 3: **Benchmark Experiments Overview.** Our study encompasses tests across eight primary model architectures, each featuring 3-4 common backbone models or composite models within its category. The figure annotates the base model parameter size for clarity. In total, **1263** experimental setups were conducted, demonstrating the adaptability of various model architectures to different task types.

- **T5 Series Excellence:** The T5 series models show excellent performance across these tasks.
- **Graph Models vs. T5 Series:** Only the significantly larger T5 series models surpass GNNs, affirming the superiority of smaller-scale graph models for molecular embedding.
- **Efficacy of Average Pooling:**

The average pooling mechanism tends to achieve superior performance more easily.

3.3 Analysis of Model Knowledge-Learning Preferences

In exploring the knowledge-learning preferences of models in the process of molecular SLM, this section introduces a language-driven, statistically significant, interpretable method. This tool constructs a token mapping matrix between input data and inference outcomes, revealing the model’s mechanism. We typically view high-frequency token mappings as indicative of specialized knowledge. Our approach identifies two types of high-frequency token mappings: general pairs, which are widespread and lack specific context, and particular pairs, essential for certain contexts but not always the most frequent. The challenge arises when standard analysis methods prioritize these general high-frequency mappings, consequently overlooking the specific ones that often carry more valuable contextual insights.

We utilize a localized feature filtering method for high-frequency selection to eliminate common high-frequency mapping pairs, thus more accurately filtering the model’s knowledge mappings. Subsequently, a significant statistical method is applied to determine the filtering threshold, identifying high-frequency mapping pairs that reflect the model’s chemical knowledge.

Proof Point 1: Sorting the matrix A in descending order by row and column totals enhances the similarity among adjacent values. Assuming each $A_{i,j}$ follows an independent and identical distribution, such as normal distribution, the row sums R_i and column sums C_j mimic this distribution. Consequently, in the sorted matrix A' , elements next to each other are more likely to come from rows or columns with similar totals.

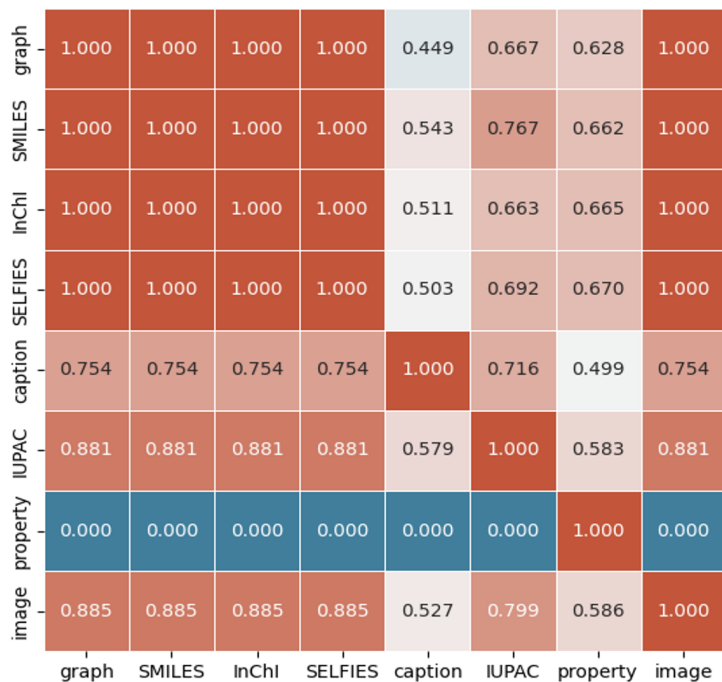
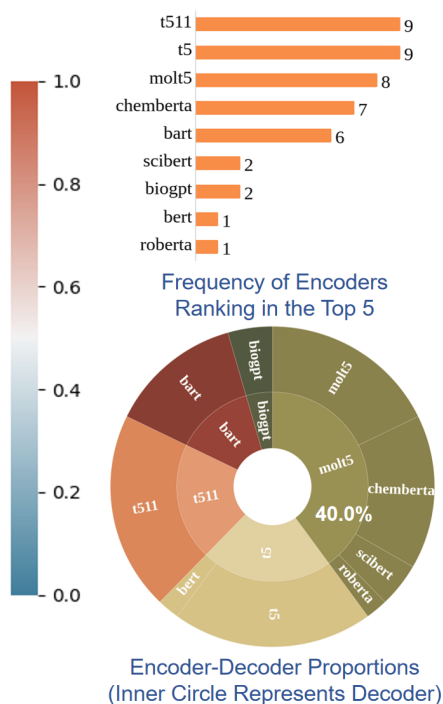
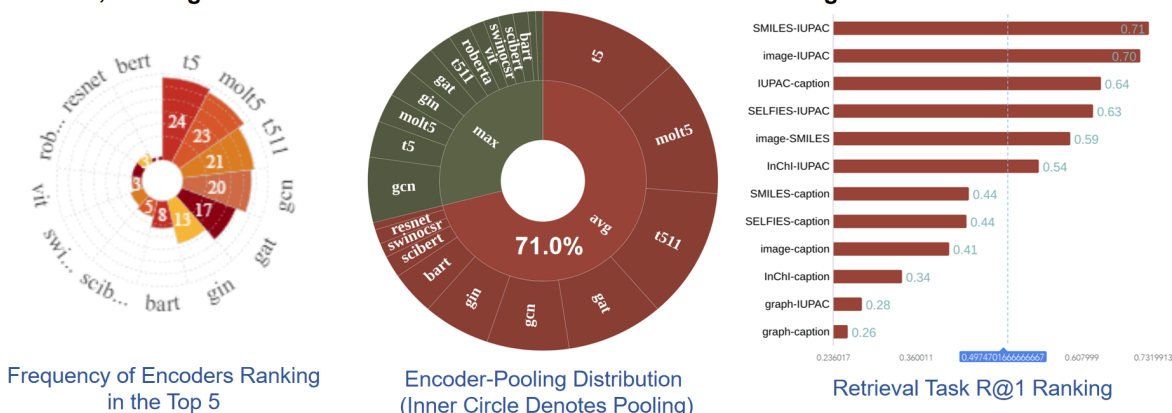
a. Modal Transition Probability Matrix**b. Encoders and Decoders in Nine Text-to-Text Tasks****c. Encoders, Pooling Mechanisms and Retrieval Performance in Embedding Tasks**

Figure 4: **Results of Benchmark.** **a. Modal Transition Probability Matrix.** This matrix presents the performance in text generation and property prediction tasks. The vertical axis represents input modalities, while the horizontal axis denotes output modalities. **b. Encoders and Decoders in Nine Text-to-Text Tasks.** This illustration highlights the frequency of various models appearing in the top 5 rankings. The T5 series models exhibit a dominant presence. **c. Encoders, Pooling Mechanisms, and Retrieval Performance in Embedding Tasks.** Alongside model rankings, the figure indicates that average pooling is a preferred choice for the pooling layer. Additionally, from a molecular retrieval perspective, SMILES-IUPAC retrieval demonstrates the highest efficiency.

Considering A'_{kl} and its neighbors $A'_{k\pm 1, l\pm 1}$ in A' , which were close in the sum in the original matrix A , the probability they are similar is mathematically represented as:

$$P(A'_{kl} \approx A'_{k\pm 1, l\pm 1} | R_i \approx R_{i\pm 1}, C_j \approx C_{j\pm 1}) > P(A_{ij} \approx A_{i\pm 1, j\pm 1})$$

This highlights that adjacent elements in A' are more likely to have close values compared to those in A , due to the sorting based on similar row and column sums.

Proof Point 2: To uncover significant patterns within a matrix, we introduce a threshold T , aiming to spotlight elements A_{ij} that significantly surpass the mean plus a certain number of standard deviations of their neighboring values. This process starts with assuming elements in matrix A are drawn from a distribution, enabling the calculation of each element’s neighborhood mean $\mu_{neighbor}$ and standard deviation $\sigma_{neighbor}$. This step evaluates whether an element exceeds the set threshold, the condition to filter elements that starkly differ from their surrounding context:

$$A_{ij} > \mu_{neighbor} + T \cdot \sigma_{neighbor}$$

To assess the actual significance of these findings, we calculate the actual proportion P_{actual} of elements exceeding this threshold across the matrix and compare it to the expected proportion $P_{expected}$ under a normal distribution. The actual and expected proportion are determined by the fraction of elements satisfying our condition:

$$P_{actual} = \frac{\sum I_{ij}}{n \times m}$$

$$P_{expected} = 1 - \Phi\left(\frac{\mu_{neighbor} + T \cdot \sigma_{neighbor} - \mu}{\sigma}\right)$$

where I_{ij} is an indicator function that equals 1 when the condition is met and 0 otherwise, and $n \times m$ represents the matrix size. The Φ represents the cumulative distribution function(CDF) of the standard normal distribution, and μ and σ are the mean and standard deviation of the entire matrix’s elements.

Finally, a statistical test, such as the Z-test, evaluates the significance of the observed proportion against the expected, indicating whether the identified patterns are indeed statistically significant beyond random chance:

$$Z = \frac{P_{actual} - P_{expected}}{\sqrt{\frac{P_{expected}(1-P_{expected})}{n \times m}}}$$

This succinct methodology not only clarifies the process of identifying statistically significant patterns but also underlines its effectiveness in distinguishing genuine high-frequency elements from those of a random distribution, offering valuable insights into the structure of the knowledge-learning preferences of models.

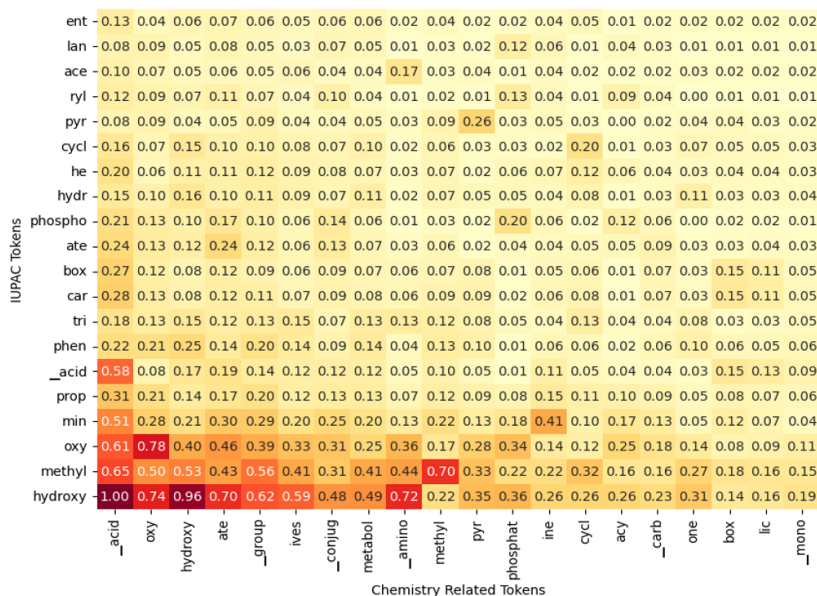
3.4 Case Studies on Model Knowledge-Learning Preferences

Our analysis aims to discern model preferences for knowledge acquisition. To enhance interpretability, we focus on the IUPAC-to-caption mapping process, which is closely aligned with natural language tasks. Figure 5. a displays the token mapping matrix after normalization and rearrangement based on the total counts of rows and columns, selecting the top 20 high-frequency chemical tokens in IUPAC names and captions. General high-frequency mappings, such as oxy, methyl, and hydroxy, appear extensively across various tokens. Traditional filtering methods might capture many of these mappings yet potentially exclude those with specific contextual significance.

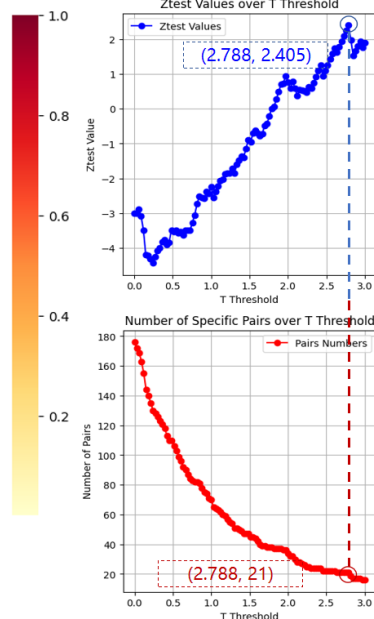
To find specific high-frequency mapping pairs, as shown in Figure 5. b, at $T = 2.788$, the Z-test reaches its maximum value of 2.405, corresponding to a confidence level of 98.2%. After identifying 21 specific token mapping pairs and removing those with identical row and column names, we are left with 16 unique pairs. By consolidating mappings with the same leading or trailing tokens, we obtain the following 9 groups of token mappings:

- ['ent'] → ['methyl']
- ['lan', 'phospho'] → ['phosphat']
- ['ace'] → ['amino']
- ['ryl'] → ['acy', 'ate', 'acid', 'conjug']
- ['hydr'] → ['one']
- ['cycl'] → ['hydroxy', 'one']
- ['phen'] → ['group']
- ['min'] → ['ine']
- ['hydroxy'] → ['acid', 'mono']

a. IUPAC-to-Caption Tokens Mapping Matrix of T5



b. Threshold T Analysis



c. Examples of T5 Knowledge-Learning Preferences.

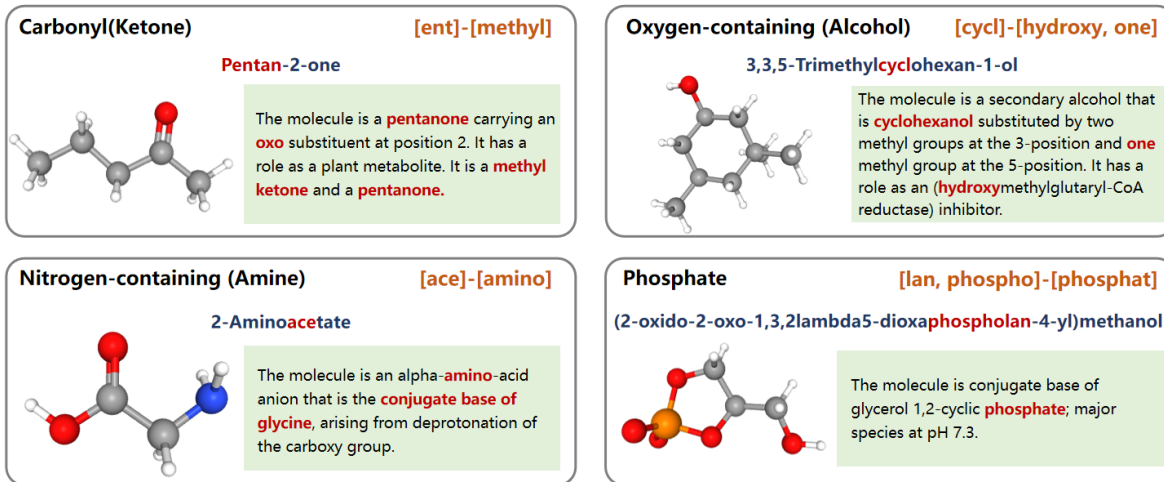


Figure 5: **Co-occurrence Patterns and Insights.** a. **IUPAC-to-Caption Tokens Mapping Matrix of T5** The matrix displays the y-axis as high-frequency tokens from IUPAC and the x-axis as chemical tokens selected from the captions. This visualization facilitates the identification of data points with high co-occurrence frequencies. b. **Threshold T Analysis.** There are 100 thresholds within the range [0,3] for T . As the threshold increases, the criteria for selecting specific high-frequency pairs become more stringent, reducing their number while also affecting significance levels. c. **Examples of T5 Knowledge-Learning Preferences.** In our IUPAC-to-caption analysis, we select four mapping patterns that reveal the model’s grasp of chemical structures and language, aligning with known chemical knowledge. (1) The mapping from ‘ent’ to ‘methyl’ demonstrates the model’s ability to identify molecular structural elements, like the carbonyl group in Pentan-2-one. (2) The ‘cycl’ to ‘hydroxy’ and ‘one’ mapping indicates the model’s understanding of complex structures, recognizing the cyclohexanol structure and hydroxyl groups in 3,3,5-Trimethylcyclohexan-1-ol. (3) Mapping ‘ace’ to ‘amino’ shows the model’s knowledge of biochemical principles, identifying the role of amino groups in 2-aminoacetate. (4) The ‘lan’ and ‘phospho’ to ‘phosphat’ mapping reveals the model’s insight into phosphate groups and their biological importance.

These mapping patterns illustrate the diversity and specificity of chemical token relationships captured through our analysis. Following these mapping patterns, we randomly select corresponding molecular IUPAC names and their captions, as shown in Figure 5. c.

The T5 model exhibits a robust understanding of molecules featuring functional groups such as carbonyls (e.g., ketones), oxygen-containing groups (e.g., alcohols), nitrogen-containing groups (e.g., amines), and phosphate groups, accurately interpreting their chemical properties and impacts on molecular characteristics. Through a series of model knowledge-learning insights, we demonstrate that the observed mapping patterns are not merely coincidental but reflective of the model’s inherent ability to process and interpret complex chemical information.

4 Discussion

The Impact of Data Modalities To identify how data modalities influence model performance in molecular science tasks, we develop a multi-modal benchmark and carry out thousands of experiments. Yet, our focus on prevalent data modalities and established backbone models may overlook some Fingerprint modalities and innovative training strategies. Therefore, our findings provide comparative insights, highlighting areas for more profound research in future work.

Scientific Insights Discovery To explore the knowledge-learning preferences, we provide an interpretable analysis, revealing the foundational mechanisms in molecular SLM. It confirms that models are capable of modeling chemical knowledge. Nevertheless, our investigation primarily adopts an NLP standpoint, with limited incorporation of scientific principles. To more clearly showcase the models’ capabilities in scientific understanding, future research should incorporate a broader spectrum of biochemical and physical chemistry knowledge.

Benchmarking of SLM While we strive to include a broad range of metrics for various tasks, our approach to molecular generation tasks primarily relies on similarity metrics in comparison to target texts. This methodology falls short in evaluating the actual volume of knowledge acquired by the models. A more comprehensive assessment framework is needed to accurately gauge the learning capabilities of these models in molecular generation.

5 Conclusion

Our study presents a comprehensive review of LLMs in molecular modeling and design. We propose a multi-modal benchmark named ChEBI-20-MM, substantiated by 1263 experiments to evaluate LLMs, with a focus on the model’s adaptability of data modalities and knowledge acquisition. We demonstrate insights into the most suitable modalities for tasks by the modal transition probability matrix. Furthermore, we utilize statistically localized feature filtering to discover model knowledge-learning preferences. These advancements lay the groundwork for future progress in molecular SLM.

In future research, we will focus on a sophisticated exploration of multi-modal data fusion to understand how various data modalities enhance model performance. We plan to tailor evaluation metrics specifically for different SLM tasks, moving beyond merely focusing on similarity to the target text. Additionally, integrating scientific perspectives, including biochemical and pharmacological analyses, will offer a more comprehensive understanding of the models’ capabilities. These steps will bridge the gap between computational modeling and practical scientific applications, unlocking new potential in molecular sciences.

Data and Software Availability:

The data and software can be accessed at <https://github.com/AI-HPC-Research-Team/SLM4Mol>. It is available for non-commercial use.

Funding

This work is supported by grants from the National Natural Science Foundation of China (61902446, 62172456, and 91937302) and the Peng Cheng Cloud-Brain of Peng Cheng Laboratory.

CRedit authorship contribution statement

Pengfei Liu: Conceptualization, Methodology, Data curation, Model training, Writing-original draft. Jun Tao: Writing review editing. Zhixiang Ren: Conceptualization, Formal analysis, Supervision, Funding acquisition, Writing review editing.

Declaration of Competing Interest

The authors declare that they have no known competing financial interests or personal relationships that could have appeared to influence the work reported in this paper.

Acknowledgment

This research was supported by the Peng Cheng Laboratory and Peng Cheng Cloud-Brain.

References

- [1] K. Heikamp and J. Bajorath, "Support vector machines for drug discovery," *Expert opinion on drug discovery*, vol. 9, no. 1, pp. 93–104, 2014.
- [2] O. Wieder, S. Kohlbacher, M. Kuenemann, A. Garon, P. Ducrot, T. Seidel, and T. Langer, "A compact review of molecular property prediction with graph neural networks," *Drug Discovery Today: Technologies*, vol. 37, pp. 1–12, 2020.
- [3] S. Liu, H. Wang, W. Liu, J. Lasenby, H. Guo, and J. Tang, "Pre-training molecular graph representation with 3d geometry," in *International Conference on Learning Representations*, 2021.
- [4] G. Zhou, Z. Gao, Q. Ding, H. Zheng, H. Xu, Z. Wei, L. Zhang, and G. Ke, "Uni-mol: A universal 3d molecular representation learning framework," in *The Eleventh International Conference on Learning Representations*, 2022.
- [5] A. Creswell, T. White, V. Dumoulin, K. Arulkumaran, B. Sengupta, and A. A. Bharath, "Generative adversarial networks: An overview," *IEEE signal processing magazine*, vol. 35, no. 1, pp. 53–65, 2018.
- [6] N. De Cao and T. Kipf, "Molgan: An implicit generative model for small molecular graphs.," in *ICML 2018 workshop on Theoretical Foundations and Applications of Deep Generative Models.*, 2018.
- [7] M. Xu, L. Yu, Y. Song, C. Shi, S. Ermon, and J. Tang, "Geodiff: A geometric diffusion model for molecular conformation generation," in *International Conference on Learning Representations*, 2021.
- [8] A. Vaswani, N. Shazeer, N. Parmar, J. Uszkoreit, L. Jones, A. N. Gomez, Ł. Kaiser, and I. Polosukhin, "Attention is all you need," *Advances in neural information processing systems*, vol. 30, 2017.
- [9] A. Radford, J. Wu, R. Child, D. Luan, D. Amodei, I. Sutskever, *et al.*, "Language models are unsupervised multitask learners," *OpenAI blog*, 2019.
- [10] OpenAI, "GPT-4 technical report," *CoRR*, vol. abs/2303.08774, 2023.
- [11] Y. Du, T. Fu, J. Sun, and S. Liu, "Molgensurvey: A systematic survey in machine learning models for molecule design," *arXiv preprint arXiv:2203.14500*, 2022.
- [12] Y. Fang, Q. Zhang, Z. Chen, X. Fan, and H. Chen, "Knowledge-informed molecular learning: A survey on paradigm transfer," *arXiv preprint arXiv:2202.10587*, 2022.
- [13] T. Guo, K. Guo, Z. Liang, Z. Guo, N. V. Chawla, O. Wiest, X. Zhang, *et al.*, "What indeed can gpt models do in chemistry? a comprehensive benchmark on eight tasks," *arXiv preprint arXiv:2305.18365*, 2023.
- [14] Y. Fang, X. Liang, N. Zhang, K. Liu, R. Huang, Z. Chen, X. Fan, and H. Chen, "Mol-instructions: A large-scale biomolecular instruction dataset for large language models," *arXiv preprint arXiv:2306.08018*, 2023.
- [15] D. Weininger, "Smiles, a chemical language and information system. 1. introduction to methodology and encoding rules," *Journal of chemical information and computer sciences*, vol. 28, no. 1, pp. 31–36, 1988.
- [16] S. Heller, A. McNaught, S. Stein, D. Tchekhovskoi, and I. Pletnev, "Inchi-the worldwide chemical structure identifier standard," *Journal of cheminformatics*, vol. 5, no. 1, pp. 1–9, 2013.
- [17] M. Krenn, F. Häse, A. Nigam, P. Friederich, and A. Aspuru-Guzik, "Self-referencing embedded strings (selfies): A 100% robust molecular string representation," *Machine Learning: Science and Technology*, vol. 1, no. 4, p. 045024, 2020.
- [18] G. L. Long and J. D. Winefordner, "Limit of detection. a closer look at the iupac definition," *Analytical chemistry*, vol. 55, no. 7, pp. 712A–724A, 1983.
- [19] S. Kim, J. Chen, T. Cheng, A. Gindulyte, J. He, S. He, Q. Li, B. A. Shoemaker, P. A. Thiessen, B. Yu, *et al.*, "Pubchem 2023 update," *Nucleic acids research*, vol. 51, no. D1, pp. D1373–D1380, 2023.

- [20] J. J. Irwin, K. G. Tang, J. Young, C. Dandarchuluun, B. R. Wong, M. Khurelbaatar, Y. S. Moroz, J. Mayfield, and R. A. Sayle, "Zinc20—a free ultralarge-scale chemical database for ligand discovery," *Journal of chemical information and modeling*, vol. 60, no. 12, pp. 6065–6073, 2020.
- [21] B. Zdrzil, E. Felix, F. Hunter, E. J. Manners, J. Blackshaw, S. Corbett, M. de Veij, H. Ioannidis, D. Mendez Lopez, J. F. Mosquera, *et al.*, "The chembl database in 2023: a drug discovery platform spanning multiple bioactivity data types and time periods," *Nucleic Acids Research*, p. gkad1004, 2023.
- [22] J. Hastings, G. Owen, A. Dekker, M. Ennis, N. Kale, V. Muthukrishnan, S. Turner, N. Swainston, P. Mendes, and C. Steinbeck, "Chebi in 2016: Improved services and an expanding collection of metabolites," *Nucleic acids research*, vol. 44, no. D1, pp. D1214–D1219, 2016.
- [23] D. S. Wishart, Y. D. Feunang, A. C. Guo, E. J. Lo, A. Marcu, J. R. Grant, T. Sajed, D. Johnson, C. Li, Z. Sayeeda, *et al.*, "Drugbank 5.0: a major update to the drugbank database for 2018," *Nucleic acids research*, vol. 46, no. D1, pp. D1074–D1082, 2018.
- [24] C. Raffel, N. Shazeer, A. Roberts, K. Lee, S. Narang, M. Matena, Y. Zhou, W. Li, and P. J. Liu, "Exploring the limits of transfer learning with a unified text-to-text transformer," *The Journal of Machine Learning Research*, vol. 21, no. 1, pp. 5485–5551, 2020.
- [25] B. Su, D. Du, Z. Yang, Y. Zhou, J. Li, A. Rao, H. Sun, Z. Lu, and J.-R. Wen, "A molecular multimodal foundation model associating molecule graphs with natural language," *arXiv preprint arXiv:2209.05481*, 2022.
- [26] D. Polykovskiy, A. Zhebrak, B. Sanchez-Lengeling, S. Golovanov, O. Tatanov, S. Belyaev, R. Kurbanov, A. Artamonov, V. Aladinskiy, M. Veselov, *et al.*, "Molecular sets (moses): a benchmarking platform for molecular generation models," *Frontiers in pharmacology*, vol. 11, p. 565644, 2020.
- [27] Z. Zeng, Y. Yao, Z. Liu, and M. Sun, "A deep-learning system bridging molecule structure and biomedical text with comprehension comparable to human professionals," *Nature communications*, vol. 13, no. 1, p. 862, 2022.
- [28] C. Edwards, C. Zhai, and H. Ji, "Text2mol: Cross-modal molecule retrieval with natural language queries," in *Proceedings of the 2021 Conference on Empirical Methods in Natural Language Processing*, pp. 595–607, 2021.
- [29] S. Liu, W. Nie, C. Wang, J. Lu, Z. Qiao, L. Liu, J. Tang, C. Xiao, and A. Anandkumar, "Multi-modal molecule structure-text model for text-based retrieval and editing," *arXiv preprint arXiv:2212.10789*, 2022.
- [30] Z. Wu, B. Ramsundar, E. N. Feinberg, J. Gomes, C. Geniesse, A. S. Pappu, K. Leswing, and V. Pande, "Moleculenet: a benchmark for molecular machine learning," *Chemical science*, vol. 9, no. 2, pp. 513–530, 2018.
- [31] "Osra validation datasets." <https://sourceforge.net/p/osra/wiki/Validation/>, 2020. Accessed: 2020-06-24.
- [32] "CLEF-IP 2012 Structure Recognition Test Set." <https://www.ifs.tuwien.ac.at/~clef-ip/download/2012/qrels/clef-ip-2012-chem-recognition-qrels.tgz>, 2012. Accessed: 2020-06-29.
- [33] "Molrecuob benchmark dataset." <https://www.cs.bham.ac.uk/research/groupings/reasoning/sdag/chemical.php>, 2020. Accessed: 2020-06-29.
- [34] N. Schneider, N. Stiefl, and G. A. Landrum, "What's what: The (nearly) definitive guide to reaction role assignment," *Journal of chemical information and modeling*, vol. 56, no. 12, pp. 2336–2346, 2016.
- [35] J. D. M.-W. C. Kenton and L. K. Toutanova, "Bert: Pre-training of deep bidirectional transformers for language understanding," in *Proceedings of NAACL-HLT*, pp. 4171–4186, 2019.
- [36] Y. Liu, M. Ott, N. Goyal, J. Du, M. Joshi, D. Chen, O. Levy, M. Lewis, L. Zettlemoyer, and V. Stoyanov, "Roberta: A robustly optimized bert pretraining approach," *arXiv preprint arXiv:1907.11692*, 2019.
- [37] I. Beltagy, K. Lo, and A. Cohan, "Scibert: A pretrained language model for scientific text," in *Proceedings of the 2019 Conference on Empirical Methods in Natural Language Processing and the 9th International Joint Conference on Natural Language Processing (EMNLP-IJCNLP)*, pp. 3615–3620, 2019.
- [38] S. Chithrananda, G. Grand, and B. Ramsundar, "Chemberta: large-scale self-supervised pretraining for molecular property prediction," *arXiv preprint arXiv:2010.09885*, 2020.
- [39] J. Schulman, B. Zoph, C. Kim, J. Hilton, J. Menick, J. Weng, J. F. C. Uribe, L. Fedus, L. Metz, M. Pokorny, *et al.*, "Chatgpt: Optimizing language models for dialogue," *OpenAI blog*, 2022.
- [40] Z. Liu, W. Zhang, Y. Xia, L. Wu, S. Xie, T. Qin, M. Zhang, and T.-Y. Liu, "Molxpt: Wrapping molecules with text for generative pre-training," *arXiv preprint arXiv:2305.10688*, 2023.
- [41] J. Li, Y. Liu, W. Fan, X.-Y. Wei, H. Liu, J. Tang, and Q. Li, "Empowering molecule discovery for molecule-caption translation with large language models: A chatgpt perspective," *arXiv preprint arXiv:2306.06615*, 2023.

- [42] M. Lewis, Y. Liu, N. Goyal, M. Ghazvininejad, A. Mohamed, O. Levy, V. Stoyanov, and L. Zettlemoyer, "Bart: Denoising sequence-to-sequence pre-training for natural language generation, translation, and comprehension," in *Proceedings of the 58th Annual Meeting of the Association for Computational Linguistics*, pp. 7871–7880, 2020.
- [43] C. Edwards, T. Lai, K. Ros, G. Honke, K. Cho, and H. Ji, "Translation between molecules and natural language," in *2022 Conference on Empirical Methods in Natural Language Processing, EMNLP 2022*, 2022.
- [44] D. Christofidellis, G. Giannone, J. Born, O. Winther, T. Laino, and M. Manica, "Unifying molecular and textual representations via multi-task language modelling," *arXiv preprint arXiv:2301.12586*, 2023.
- [45] J. Li, D. Li, S. Savarese, and S. Hoi, "Blip-2: Bootstrapping language-image pre-training with frozen image encoders and large language models," *arXiv preprint arXiv:2301.12597*, 2023.
- [46] D. Zhu, J. Chen, X. Shen, X. Li, and M. Elhoseiny, "Minigt-4: Enhancing vision-language understanding with advanced large language models," *arXiv preprint arXiv:2304.10592*, 2023.
- [47] P. Liu, Y. Ren, and Z. Ren, "Git-mol: A multi-modal large language model for molecular science with graph, image, and text," *arXiv preprint arXiv:2308.06911*, 2023.
- [48] P. Seidl, A. Vall, S. Hochreiter, and G. Klambauer, "Enhancing activity prediction models in drug discovery with the ability to understand human language," *arXiv preprint arXiv:2303.03363*, 2023.
- [49] J. Zhu, Y. Xia, L. Wu, S. Xie, W. Zhou, T. Qin, H. Li, and T.-Y. Liu, "Dual-view molecular pre-training," in *Proceedings of the 29th ACM SIGKDD Conference on Knowledge Discovery and Data Mining*, pp. 3615–3627, 2023.
- [50] J. Ross, B. Belgodere, V. Chenthamarakshan, I. Padhi, Y. Mroueh, and P. Das, "Large-scale chemical language representations capture molecular structure and properties," *Nature Machine Intelligence*, vol. 4, no. 12, pp. 1256–1264, 2022.
- [51] Z. Guo, P. Sharma, A. Martinez, L. Du, and R. Abraham, "Multilingual molecular representation learning via contrastive pre-training," in *Proceedings of the 60th Annual Meeting of the Association for Computational Linguistics (Volume 1: Long Papers)*, pp. 3441–3453, 2022.
- [52] J. Jiang, R. Zhang, Y. Yuan, T. Li, G. Li, Z. Zhao, and Z. Yu, "Noisemol: A noise-robusted data augmentation via perturbing noise for molecular property prediction," *Journal of Molecular Graphics and Modelling*, vol. 121, p. 108454, 2023.
- [53] J. Gao, Z. Shen, Y. Xie, J. Lu, Y. Lu, S. Chen, Q. Bian, Y. Guo, L. Shen, J. Wu, *et al.*, "Transfoxmol: predicting molecular property with focused attention," *Briefings in Bioinformatics*, p. bbad306, 2023.
- [54] C. Ying, T. Cai, S. Luo, S. Zheng, G. Ke, D. He, Y. Shen, and T.-Y. Liu, "Do transformers really perform badly for graph representation?," *Advances in Neural Information Processing Systems*, vol. 34, pp. 28877–28888, 2021.
- [55] A. Xie, Z. Zhang, J. Guan, and S. Zhou, "Self-supervised learning with chemistry-aware fragmentation for effective molecular property prediction," *Briefings in Bioinformatics*, p. bbad296, 2023.
- [56] E. Mazuz, G. Shtar, B. Shapira, and L. Rokach, "Molecule generation using transformers and policy gradient reinforcement learning," *Scientific Reports*, vol. 13, no. 1, p. 8799, 2023.
- [57] Y. Fang, N. Zhang, Z. Chen, X. Fan, and H. Chen, "Domain-agnostic molecular generation with self-feedback," 2023.
- [58] D. Rothchild, A. Tamkin, J. Yu, U. Misra, and J. Gonzalez, "C5t5: Controllable generation of organic molecules with transformers," *arXiv preprint arXiv:2108.10307*, 2021.
- [59] J. Lu and Y. Zhang, "Unified deep learning model for multitask reaction predictions with explanation," *Journal of Chemical Information and Modeling*, p. 1376–1387, Mar 2022.
- [60] M. Livne, Z. Miftahutdinov, E. Tutubalina, M. Kuznetsov, D. Polykovskiy, A. Brundyn, A. Jhunjhunwala, A. Costa, A. Aliper, and A. Zhavoronkov, "nach0: Multimodal natural and chemical languages foundation model," *arXiv preprint arXiv:2311.12410*, 2023.
- [61] J. He, F. Mattsson, M. Forsberg, E. J. Bjerrum, O. Engkvist, C. Tyrchan, W. Czechtizky, *et al.*, "Transformer neural network for structure constrained molecular optimization," *Journal of Cheminformatics*, 2022.
- [62] A. M. Bran, S. Cox, A. D. White, and P. Schwaller, "Chemcrow: Augmenting large-language models with chemistry tools," *arXiv preprint arXiv:2304.05376*, 2023.
- [63] X. Tang, A. Tran, J. Tan, and M. Gerstein, "Mollm: Integrating 3d and 2d molecular representations with biomedical text via a unified pre-trained language model," *bioRxiv*, pp. 2023–11, 2023.
- [64] Y. Luo, K. Yang, M. Hong, X. Liu, and Z. Nie, "Molfm: A multimodal molecular foundation model," *arXiv preprint arXiv:2307.09484*, 2023.

- [65] Z. Liu, S. Li, Y. Luo, H. Fei, Y. Cao, K. Kawaguchi, X. Wang, and T.-S. Chua, "Molca: Molecular graph-language modeling with cross-modal projector and uni-modal adapter," in *Proceedings of the 2023 Conference on Empirical Methods in Natural Language Processing*, pp. 15623–15638, 2023.
- [66] R. Taylor, M. Kardas, G. Cucurull, T. Scialom, A. Hartshorn, E. Saravia, A. Poulton, V. Kerkez, and R. Stojnic, "Galactica: A large language model for science," *arXiv preprint arXiv:2211.09085*, 2022.
- [67] L. Krasnov, I. Khokhlov, M. Fedorov, and S. Sosnin, "Struct2iupac–transformer-based artificial neural network for the conversion between chemical notations," *Scientific Reports*, 2021.
- [68] J. Mao, J. Wang, A. Zeb, K.-H. Cho, H. Jin, J. Kim, O. Lee, Y. Wang, and K. T. No, "Transformer-based molecular generative model for antiviral drug design," *Journal of Chemical Information and Modeling*, 2023.
- [69] C. Qian, H. Tang, Z. Yang, H. Liang, and Y. Liu, "Can large language models empower molecular property prediction?," *arXiv preprint arXiv:2307.07443*, 2023.
- [70] K. Rajan, A. Zielesny, and C. Steinbeck, "Decimer 1.0: deep learning for chemical image recognition using transformers," *Journal of Cheminformatics*, vol. 13, no. 1, pp. 1–16, 2021.
- [71] I. Khokhlov, L. Krasnov, M. V. Fedorov, and S. Sosnin, "Image2smiles: Transformer-based molecular optical recognition engine," *Chemistry-Methods*, vol. 2, no. 1, p. e202100069, 2022.
- [72] J. Yi, C. Wu, X. Zhang, X. Xiao, Y. Qiu, W. Zhao, T. Hou, and D. Cao, "Micer: a pre-trained encoder-decoder architecture for molecular image captioning," *Bioinformatics (Oxford, England)*, vol. 38, no. 19, pp. 4562–4572, 2022.
- [73] Z. Xu, J. Li, Z. Yang, S. Li, and H. Li, "Swinocrs: end-to-end optical chemical structure recognition using a swin transformer," *Journal of Cheminformatics*, vol. 14, no. 1, pp. 1–13, 2022.
- [74] Z. Liu, Y. Lin, Y. Cao, H. Hu, Y. Wei, Z. Zhang, S. Lin, and B. Guo, "Swin transformer: Hierarchical vision transformer using shifted windows," in *Proceedings of the IEEE/CVF international conference on computer vision*, pp. 10012–10022, 2021.
- [75] Y. Qian, J. Guo, Z. Tu, Z. Li, C. W. Coley, and R. Barzilay, "Molscribe: Robust molecular structure recognition with image-to-graph generation," *Journal of Chemical Information and Modeling*, vol. 63, no. 7, pp. 1925–1934, 2023.
- [76] Q. Pei, W. Zhang, J. Zhu, K. Wu, K. Gao, L. Wu, Y. Xia, and R. Yan, "Biot5: Enriching cross-modal integration in biology with chemical knowledge and natural language associations," in *Proceedings of the 2023 Conference on Empirical Methods in Natural Language Processing*, pp. 1102–1123, 2023.
- [77] V. Bagal, R. Aggarwal, P. Vinod, and U. D. Priyakumar, "Molgpt: molecular generation using a transformer-decoder model," *Journal of Chemical Information and Modeling*, vol. 62, no. 9, pp. 2064–2076, 2021.
- [78] R. Irwin, S. Dimitriadis, J. He, and E. J. Bjerrum, "Chemformer: a pre-trained transformer for computational chemistry," *Machine Learning: Science and Technology*, vol. 3, no. 1, p. 015022, 2022.
- [79] Z. Zeng, B. Yin, S. Wang, J. Liu, C. Yang, H. Yao, X. Sun, M. Sun, G. Xie, and Z. Liu, "Interactive molecular discovery with natural language," *arXiv preprint arXiv:2306.11976*, 2023.

Appendix

A. The Details of Models

An overview of model classifications and architectures is shown in Table 2.

Table 2: Overview of models in molecular modeling design categorized by their architecture and backbone. The abbreviations **MC**, **INR**, **MPP**, **MR**, **MIR**, **MG**, and **OT** correspond to the tasks investigated: molecule captioning, IUPAC name recognition, molecular property prediction, molecular retrieval, molecular image recognition, molecule generation, and other tasks, respectively. Each ● symbol in the table denotes the demonstrated task capabilities of the models as reported in their publications. Notably, the ● symbol specifically signifies the specialized task of molecular optimization within the broader context of molecule generation.

Architecture	Backbone	Model	Date	MC	INR	MPP	MR	MIR	MG	OT
Encoder-only	BERT	KV-PLM [27]	2022/02			●	●			●
		CLAMP [48]	2023/05			●				
	RoBERTa	ChemBERTa [38]	2020/10			●				
		DMP [49]	2021/10			●				
	Transformer	Molformer [50]	2022/04			●	●			
Graphormer [54]	MM-Deacon [51]	2022/04			●					
	NoiseMol [52]	2023/01			●					
Decoder-only	GPT	TransFoxMol [53]	2023/01			●				
		CAFE-MPP [55]	2023/01			●				
		MolGPT [77]	2021/10			●			●	
	Transformer	Galactica [66]	2022/12			●				●
		MolXPT [40]	2023/05	●		●			●	
ChatGPT	Taiga [56]	2023/05						●		
Text-Text	BART [42]	MolReGPT [41]	2023/06	●					●	
		LLM4Mol [69]	2023/07			●				
	T5	Chemformer [78]	2022/02						●	
		MolGen [57]	2023/05						●	
		C5T5 [58]	2021/08						●	
		T5Chem [59]	2022/03						●	●
		MolT5 [43]	2022/11	●					●	
		Text+Chem T5[44]	2023/05	●					●	●
		ChatMol [79]	2023/06	●					●	
	TransAntivirus [68]	2023/06		●				●		
Transformer	BioT5 [76]	2023/10	●		●			●		
	nach0 [60]	2023/11	●		●			●	●	
Image-Text	Swin Transformer [74]	Struct2IUPAC [67]	2020/11		●				●	
		Transformer-R [61]	2021/04						●	
	ChemCrow[62]	2023/04						●	●	
Graph-Text	Sci-BERT	SwinOCSR [73]	2022/07					●		
		MolScribe [75]	2023/03					●		
	Transformer	DECIMER1.0 [70]	2021/08					●		
Image-Graph-Text	Q-Former [45]	Image2SMILES[71]	2022/01					●		
		MICER [72]	2022/08					●		
	Q-Former [45]	Text2Mol [28]	2021/09	●		●	●		●	
		MoMu [25]	2022/09	●		●	●		●	
	MegaMolBART [78]	MoleculeSTM [29]	2022/12			●	●		●	
Q-Former [45]	BERT	MolFM [64]	2023/07	●		●	●		●	
	KV-PLM	MolCA [65]	2023/11	●	●	●	●		●	
Image-Graph-Text	Q-Former	MolLM [63]	2023/12	●		●	●		●	
		GIT-Mol [47]	2023/08	●		●		●	●	

B. ChEBI-20-MM

In our study, we employ visualization techniques to analyze the **suitability** of data sources for language models and **chemical space coverage**. As shown in Figure 6, we use different visualization methods to analyze the distribution of text lengths and the number of tokens generated by each model’s tokenizer for various text data types. This approach allows us to evaluate the adaptability of language models to the textual characteristics of our dataset. We also focus on the top 10 scaffolds within the dataset, counting the number of molecules for each scaffold. Here, semi-transparent bars represent the total count, while solid bars indicate the quantity in the training set. On the other hand, for the analysis of **chemical space coverage**, we choose molecular weight (MW), LogP, the number of aromatic rings, and the Topological

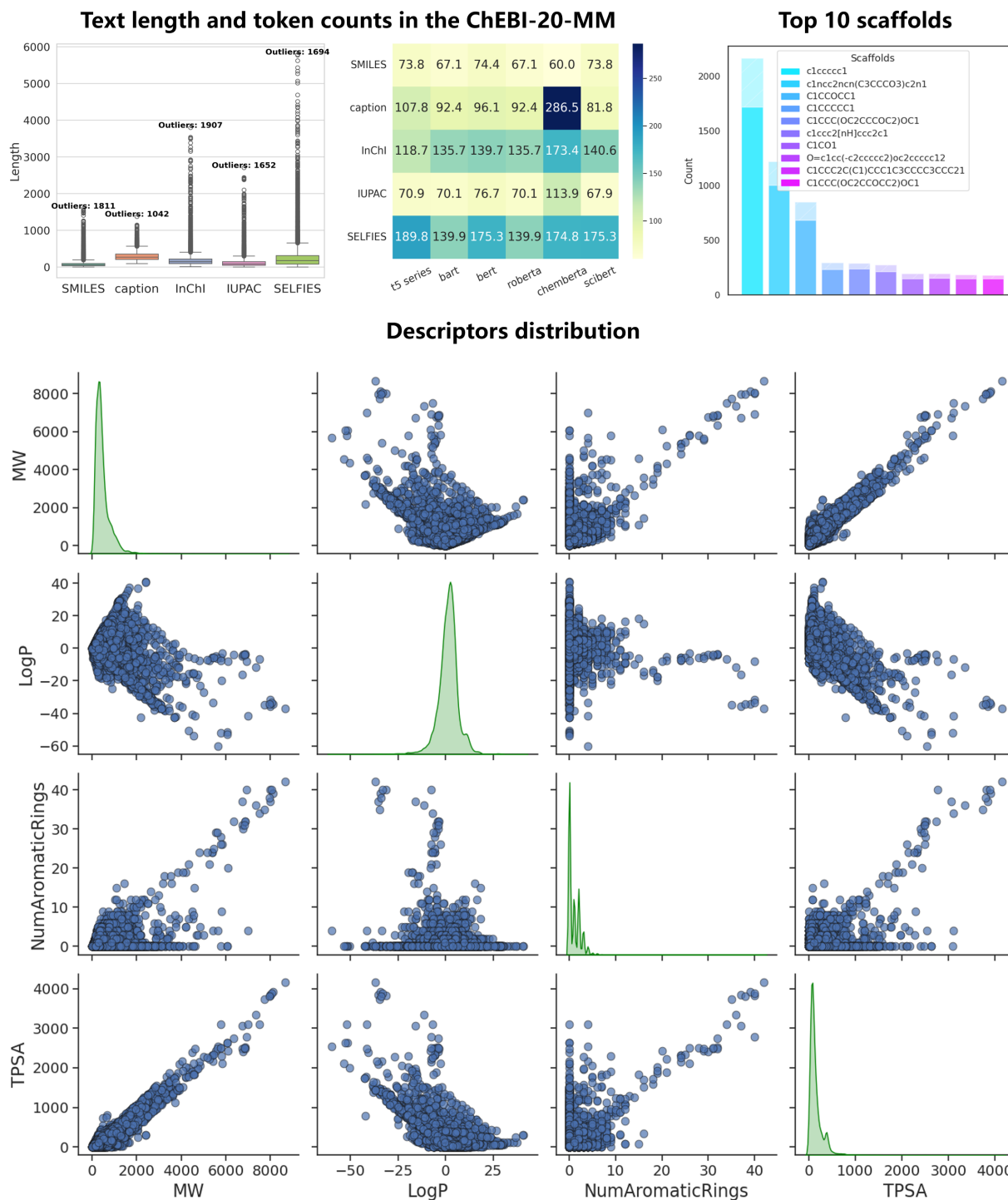


Figure 6: Visualization of Data Source Suitability and Chemical Space Diversity.

Polar Surface Area (TPSA) as descriptors. We examine the distribution and correlation of these descriptors within the dataset, providing insights into the chemical diversity and complexity present in our data.

A benchmark must exhibit a balanced distribution, preventing biases toward any specific molecular representation. Analyzing the distribution of text lengths and tokenizer outputs helps confirm that a language model's tokenizer

captures molecular information effectively. Moreover, the diversity in scaffold distribution is crucial for determining the benchmark’s generalization across chemical spaces, ensuring the language model can learn and predict a wide array of chemical entities. Finally, the distribution and correlation of molecular descriptors reveal the complexity within the chemical space. Overall, the visual analyses of text length, scaffold count, and descriptor statistics provide insights into the dataset’s characteristics, affirming the benchmark’s robustness for tasks in molecular science.

As for the metrics, we use a combination of BLEU-2, BLEU-4, ROUGE-1, ROUGE-2, ROUGE-L, and METEOR scores for IUPAC name recognition and molecule captioning. Moreover, for image recognition and molecule generation, we assess models using BLEU for textual similarity, Exact Match for precision, Valid for chemical validity of generated molecules, Levenshtein distance for structural similarity, and fingerprint-based metrics such as MACCS, RDKit², and Morgan for capturing chemical feature representation. Molecular Retrieval is evaluated using Mean Reciprocal Rank (MRR), and Recall at K (R@1, R@5, R@10). For the property prediction metrics, We utilize widely-recognized classification and regression tasks from MoleculeNet. For classification, we measure the area under the receiver operating characteristic curve (roc_auc), the area under the precision-recall curve (pr_auc), and the mean F1 score (f1_score). For regression tasks, we use mean squared error (mse_mean), root mean squared error (rmse_mean), and mean absolute error (mae_mean) to assess the predictive accuracy of the models quantitatively.

C. Experimental Results

SMILES Generation. Table 3 illustrates the performance of SMILES generation across two methodologies: image recognition and text-based SMILES generation. The image recognition task is an essential task for chemical image understanding. The results show that models leveraging Swin Transformer (SwinOCSR) for encoding and t5 for decoding effectively generate SMILES from visual inputs.

Table 3: Experimental Results for SMILES Generation

Task	Input	Encoder	Decoder	Bleu \uparrow	Exact Match \uparrow	Levenshtein \downarrow	MACCS \uparrow	RDKit \uparrow	Morgan \uparrow	Validity \uparrow
image recognition (SMILES)	image	swinocsr	t5	0.885	0.356	12.746	0.951	0.890	0.868	0.908
	image	swinocsr	t511	0.833	0.175	18.589	0.897	0.785	0.765	0.761
	image	vit	t5	0.826	0.179	19.802	0.889	0.780	0.734	0.873
	image	swin	t5	0.782	0.067	24.726	0.794	0.633	0.581	0.891
	image	swin	t511	0.779	0.066	25.203	0.802	0.648	0.597	0.850
molecule generation (text-based)	IUPAC	t5	t5	0.881	0.327	14.209	0.909	0.811	0.773	0.905
	IUPAC	t511	t511	0.881	0.323	14.141	0.911	0.808	0.771	0.893
	IUPAC	molt5	molt5	0.853	0.206	17.645	0.881	0.758	0.723	0.773
	IUPAC	scibert	molt5	0.614	0.054	51.003	0.772	0.590	0.526	0.680
	IUPAC	bert	t5	0.296	0.000	96.484	0.409	0.268	0.128	0.988
	caption	molt5	molt5	0.754	0.090	28.034	0.808	0.673	0.594	0.837
	caption	t5	t5	0.691	0.097	34.891	0.814	0.677	0.600	0.858
	caption	t511	t511	0.649	0.110	40.569	0.819	0.687	0.608	0.857
	caption	scibert	molt5	0.543	0.012	57.118	0.670	0.492	0.431	0.693
caption	chemberta	molt5	0.425	0.002	73.061	0.561	0.408	0.325	0.740	

Within the text-based SMILES generation, the combination of IUPAC nomenclature with the t5 model emerges as the most effective, highlighting the model’s ability to process and convert complex chemical language into accurate SMILES structures. Moreover, the molt5 model’s superior performance in generating molecules from captions suggests that its pre-training on SMILES expressions is advantageous for this specific task, emphasizing the value of domain-specific pre-training in enhancing model performance.

IUPAC Generation. Table 4 emphasizes the tasks associated with IUPAC Generation, focusing on the recognition of IUPAC names from molecular images and internal information. Our benchmark does not include experiments for generating IUPAC names from captions because some captions already contain IUPAC names.

For IUPAC name recognition from the molecular images, the combination of swinocsr and t5 models yields the best performance, similar to the SMILES generation task. It suggests that the swinocsr, originally pre-trained on molecular SMILES and images, is also adept at transfer learning for IUPAC name recognition tasks. On the other hand, combining SMILES data with the t5 model achieves the best results for IUPAC recognition based on molecular internal information. Although graph-based models show only slightly lower performance in textual similarity metrics compared to language models, they exhibit a relative shortfall in achieving exact matches.

²<https://www.rdkit.org/>

Table 4: Experimental Results for IUPAC and Caption Generation

Task	Input	Encoder	Decoder	Bleu-2 \uparrow	Bleu-4 \uparrow	Rouge-1 \uparrow	Rouge-2 \uparrow	Rouge-L \uparrow	Meteor-score \uparrow	Exact Match \uparrow
IUPAC recognition (image)	image	swinocsr	t5	0.820	0.758	0.781	0.621	0.740	0.799	0.220
	image	swinocsr	molt5	0.803	0.730	0.751	0.573	0.707	0.777	0.158
	image	swinocsr	t511	0.800	0.730	0.757	0.577	0.711	0.779	0.170
	image	vit	t511	0.745	0.655	0.657	0.445	0.603	0.677	0.088
	image	vit	molt5	0.725	0.632	0.644	0.431	0.589	0.667	0.069
IUPAC recognition	SMILES	t5	t5	0.820	0.755	0.751	0.573	0.703	0.767	0.210
	SMILES	t511	t511	0.794	0.719	0.711	0.515	0.660	0.732	0.146
	SMILES	chemberta	molt5	0.786	0.710	0.717	0.524	0.669	0.739	0.134
	SMILES	molt5	molt5	0.752	0.665	0.669	0.459	0.615	0.688	0.095
	SMILES	bart	bart	0.598	0.500	0.684	0.463	0.624	0.676	0.170
	InChI	t5	t5	0.744	0.658	0.648	0.442	0.591	0.663	0.131
	InChI	t511	t511	0.728	0.636	0.622	0.410	0.565	0.641	0.088
	InChI	molt5	molt5	0.728	0.635	0.622	0.413	0.566	0.642	0.093
	InChI	chemberta	molt5	0.646	0.541	0.550	0.326	0.493	0.574	0.037
	InChI	roberta	molt5	0.620	0.505	0.494	0.249	0.429	0.509	0.012
	SELFIES	molt5	molt5	0.751	0.666	0.665	0.458	0.611	0.687	0.111
	SELFIES	t5	t5	0.744	0.658	0.668	0.465	0.615	0.692	0.132
	SELFIES	t511	t511	0.720	0.633	0.655	0.440	0.601	0.677	0.097
	SELFIES	biogpt	biogpt	0.669	0.585	0.594	0.391	0.534	0.602	0.005
	SELFIES	bart	bart	0.550	0.433	0.568	0.311	0.501	0.569	0.063
	graph	gcn	t511	0.719	0.643	0.640	0.436	0.591	0.667	0.056
	graph	gat	t5	0.708	0.630	0.620	0.420	0.572	0.652	0.046
	graph	gat	t511	0.685	0.603	0.597	0.393	0.550	0.628	0.037
	graph	gin	t5	0.682	0.600	0.615	0.403	0.558	0.653	0.052
	graph	gin	molt5	0.662	0.580	0.605	0.395	0.555	0.643	0.029
	caption	t511	t511	0.736	0.665	0.707	0.532	0.660	0.716	0.185
	caption	biogpt	biogpt	0.718	0.655	0.650	0.479	0.605	0.673	0.000
	caption	molt5	molt5	0.699	0.615	0.652	0.460	0.604	0.667	0.129
	caption	t5	t5	0.621	0.545	0.675	0.495	0.627	0.679	0.183
	caption	scibert	molt5	0.596	0.503	0.531	0.314	0.478	0.568	0.025
molecule captioning	IUPAC	t5	t5	0.547	0.457	0.629	0.476	0.566	0.579	/
	IUPAC	t511	t511	0.535	0.446	0.622	0.469	0.559	0.571	/
	IUPAC	molt5	molt5	0.525	0.433	0.612	0.455	0.549	0.556	/
	IUPAC	bart	bart	0.455	0.352	0.568	0.391	0.489	0.484	/
	IUPAC	chemberta	molt5	0.424	0.333	0.550	0.386	0.492	0.490	/
	SMILES	molt5	molt5	0.535	0.436	0.625	0.466	0.559	0.563	/
	SMILES	t5	t5	0.508	0.414	0.605	0.446	0.545	0.543	/
	SMILES	t511	t511	0.488	0.392	0.586	0.426	0.528	0.522	/
	SMILES	chemberta	molt5	0.488	0.388	0.578	0.417	0.522	0.520	/
	SMILES	bart	bart	0.406	0.301	0.538	0.359	0.465	0.443	/
	InChI	t5	t5	0.477	0.383	0.577	0.415	0.518	0.511	/
	InChI	t511	t511	0.464	0.369	0.567	0.404	0.510	0.499	/
	InChI	molt5	molt5	0.461	0.367	0.571	0.406	0.513	0.500	/
	InChI	chemberta	molt5	0.451	0.356	0.557	0.394	0.502	0.490	/
	InChI	bart	bart	0.393	0.284	0.519	0.335	0.447	0.429	/
	SELFIES	t5	t5	0.462	0.360	0.569	0.400	0.506	0.503	/
	SELFIES	t511	t511	0.446	0.348	0.559	0.392	0.499	0.490	/
	SELFIES	chemberta	molt5	0.439	0.340	0.549	0.381	0.491	0.478	/
	SELFIES	bart	bart	0.377	0.266	0.510	0.320	0.434	0.414	/
	SELFIES	biogpt	biogpt	0.277	0.204	0.425	0.250	0.355	0.345	/
	graph	gat	molt5	0.419	0.318	0.521	0.345	0.460	0.449	/
	graph	gin	molt5	0.407	0.305	0.512	0.332	0.450	0.437	/
	graph	gcn	molt5	0.392	0.291	0.512	0.333	0.450	0.430	/
	graph	gin	t511	0.362	0.256	0.479	0.295	0.418	0.401	/
	graph	gcn	bart	0.358	0.251	0.489	0.298	0.413	0.391	/
image	swinocsr	molt5	0.495	0.399	0.590	0.429	0.532	0.527	/	
image	swinocsr	t511	0.492	0.394	0.585	0.422	0.527	0.524	/	
image	swinocsr	t5	0.417	0.317	0.533	0.361	0.472	0.461	/	
image	swin	molt5	0.409	0.307	0.517	0.343	0.460	0.442	/	
image	swin	t511	0.400	0.301	0.517	0.344	0.461	0.435	/	

Molecule Captioning. The molecular captions encapsulate the essence of the molecule along with its biochemical and physicochemical properties. Molecule captioning involves the conversion of various representation forms into captions. As shown in Table 4, unlike image recognition tasks for SMILES and IUPAC names, experiments on caption generation show that performance based on IUPAC and SMILES outperforms those based on image-derived captions. It suggests that image encoders excel at distilling key points from images. However, as the diversity of generated content increases and the length of the generated sequences extends, the performance of image encoder models tends to fall short of language models. Within the scope of language models, text description generation based on IUPAC is superior, partly because the target captions commonly include IUPAC names. Additionally, graph encoders exhibit

Table 5: Experimental Results for Retrieval

Task	Input	Encoder	Pooling	Target Modality	R@1 \uparrow	MRR \uparrow	R@5 \uparrow	R@10 \uparrow
molecular retrieval (caption)	IUPAC	t5	max	caption	0.637 \pm 0.024	0.741 \pm 0.022	0.880 \pm 0.019	0.936 \pm 0.012
	IUPAC	scibert	avg	caption	0.635 \pm 0.084	0.736 \pm 0.076	0.870 \pm 0.063	0.935 \pm 0.051
	IUPAC	scibert	max	caption	0.581 \pm 0.061	0.694 \pm 0.056	0.848 \pm 0.046	0.918 \pm 0.036
	IUPAC	molt5	avg	caption	0.578 \pm 0.026	0.701 \pm 0.026	0.869 \pm 0.027	0.931 \pm 0.016
	IUPAC	t5	avg	caption	0.564 \pm 0.035	0.685 \pm 0.034	0.855 \pm 0.032	0.923 \pm 0.022
	SMILES	bart	avg	caption	0.440 \pm 0.043	0.589 \pm 0.043	0.797 \pm 0.044	0.895 \pm 0.033
	SMILES	t5	max	caption	0.437 \pm 0.046	0.588 \pm 0.046	0.800 \pm 0.045	0.892 \pm 0.028
	SMILES	t5	avg	caption	0.427 \pm 0.056	0.583 \pm 0.056	0.797 \pm 0.056	0.897 \pm 0.037
	SMILES	roberta	max	caption	0.426 \pm 0.070	0.572 \pm 0.075	0.772 \pm 0.082	0.880 \pm 0.066
	SMILES	molt5	avg	caption	0.402 \pm 0.054	0.557 \pm 0.055	0.772 \pm 0.059	0.875 \pm 0.037
	InChI	t5	avg	caption	0.339 \pm 0.033	0.504 \pm 0.036	0.733 \pm 0.040	0.858 \pm 0.030
	InChI	scibert	avg	caption	0.337 \pm 0.076	0.498 \pm 0.095	0.719 \pm 0.121	0.843 \pm 0.111
	InChI	t511	avg	caption	0.325 \pm 0.053	0.488 \pm 0.062	0.717 \pm 0.077	0.846 \pm 0.062
	InChI	bart	avg	caption	0.289 \pm 0.036	0.444 \pm 0.045	0.661 \pm 0.059	0.808 \pm 0.051
	InChI	molt5	avg	caption	0.280 \pm 0.055	0.433 \pm 0.064	0.646 \pm 0.079	0.790 \pm 0.068
	SELFIES	roberta	max	caption	0.436 \pm 0.079	0.579 \pm 0.081	0.778 \pm 0.086	0.875 \pm 0.069
	SELFIES	scibert	max	caption	0.406 \pm 0.053	0.553 \pm 0.057	0.757 \pm 0.063	0.875 \pm 0.051
	SELFIES	bert	max	caption	0.393 \pm 0.055	0.546 \pm 0.063	0.751 \pm 0.073	0.868 \pm 0.062
	SELFIES	bart	avg	caption	0.367 \pm 0.053	0.520 \pm 0.057	0.731 \pm 0.065	0.853 \pm 0.055
	SELFIES	molt5	max	caption	0.339 \pm 0.041	0.492 \pm 0.045	0.709 \pm 0.054	0.835 \pm 0.045
	graph	gat	max	caption	0.259 \pm 0.060	0.406 \pm 0.079	0.610 \pm 0.111	0.765 \pm 0.111
	graph	gcn	max	caption	0.242 \pm 0.048	0.383 \pm 0.059	0.576 \pm 0.077	0.724 \pm 0.068
	graph	gin	max	caption	0.241 \pm 0.030	0.384 \pm 0.040	0.577 \pm 0.053	0.732 \pm 0.053
	graph	gat	avg	caption	0.189 \pm 0.046	0.319 \pm 0.068	0.501 \pm 0.102	0.648 \pm 0.108
	graph	gin	avg	caption	0.185 \pm 0.038	0.309 \pm 0.058	0.476 \pm 0.086	0.630 \pm 0.099
	image	swinocr	max	caption	0.411 \pm 0.124	0.552 \pm 0.146	0.748 \pm 0.181	0.844 \pm 0.164
	image	swinocr	avg	caption	0.384 \pm 0.094	0.534 \pm 0.106	0.747 \pm 0.127	0.856 \pm 0.107
	image	resnet	avg	caption	0.233 \pm 0.041	0.385 \pm 0.055	0.587 \pm 0.075	0.753 \pm 0.073
image	vit	max	caption	0.164 \pm 0.045	0.285 \pm 0.068	0.443 \pm 0.099	0.607 \pm 0.116	
image	vit	avg	caption	0.121 \pm 0.019	0.239 \pm 0.034	0.399 \pm 0.056	0.574 \pm 0.070	
molecular retrieval (IUPAC)	SMILES	t5	avg	IUPAC	0.709 \pm 0.069	0.817 \pm 0.054	0.958 \pm 0.033	0.986 \pm 0.015
	SMILES	t511	max	IUPAC	0.698 \pm 0.116	0.802 \pm 0.096	0.941 \pm 0.065	0.975 \pm 0.032
	SMILES	scibert	avg	IUPAC	0.681 \pm 0.147	0.789 \pm 0.127	0.930 \pm 0.097	0.967 \pm 0.060
	SMILES	t511	avg	IUPAC	0.655 \pm 0.099	0.775 \pm 0.082	0.930 \pm 0.055	0.970 \pm 0.028
	SMILES	bart	max	IUPAC	0.629 \pm 0.090	0.759 \pm 0.075	0.935 \pm 0.051	0.978 \pm 0.025
	InChI	t5	avg	IUPAC	0.545 \pm 0.064	0.687 \pm 0.059	0.877 \pm 0.054	0.945 \pm 0.028
	InChI	t5	max	IUPAC	0.519 \pm 0.074	0.661 \pm 0.065	0.850 \pm 0.051	0.931 \pm 0.031
	InChI	t511	avg	IUPAC	0.518 \pm 0.114	0.665 \pm 0.111	0.867 \pm 0.106	0.936 \pm 0.073
	InChI	bart	avg	IUPAC	0.502 \pm 0.085	0.662 \pm 0.084	0.882 \pm 0.085	0.950 \pm 0.049
	InChI	t511	max	IUPAC	0.499 \pm 0.099	0.654 \pm 0.094	0.868 \pm 0.090	0.945 \pm 0.046
	SELFIES	t511	max	IUPAC	0.626 \pm 0.068	0.753 \pm 0.057	0.920 \pm 0.038	0.972 \pm 0.021
	SELFIES	bart	avg	IUPAC	0.603 \pm 0.094	0.731 \pm 0.083	0.906 \pm 0.067	0.962 \pm 0.038
	SELFIES	t5	avg	IUPAC	0.570 \pm 0.076	0.706 \pm 0.069	0.887 \pm 0.059	0.950 \pm 0.035
	SELFIES	bart	max	IUPAC	0.508 \pm 0.095	0.662 \pm 0.094	0.876 \pm 0.097	0.947 \pm 0.063
	SELFIES	molt5	avg	IUPAC	0.506 \pm 0.112	0.643 \pm 0.112	0.828 \pm 0.114	0.912 \pm 0.080
	graph	gcn	max	IUPAC	0.279 \pm 0.067	0.421 \pm 0.084	0.621 \pm 0.113	0.756 \pm 0.107
	graph	gin	max	IUPAC	0.272 \pm 0.068	0.423 \pm 0.088	0.631 \pm 0.118	0.773 \pm 0.114
	graph	gin	avg	IUPAC	0.216 \pm 0.071	0.352 \pm 0.104	0.536 \pm 0.152	0.684 \pm 0.169
	graph	gat	avg	IUPAC	0.204 \pm 0.074	0.336 \pm 0.112	0.518 \pm 0.170	0.669 \pm 0.191
	graph	gcn	avg	IUPAC	0.186 \pm 0.030	0.321 \pm 0.046	0.500 \pm 0.068	0.661 \pm 0.080
	image	swin	max	IUPAC	0.696 \pm 0.083	0.803 \pm 0.069	0.945 \pm 0.050	0.979 \pm 0.030
	image	swin	avg	IUPAC	0.462 \pm 0.104	0.608 \pm 0.105	0.808 \pm 0.104	0.900 \pm 0.076
	image	resnet	avg	IUPAC	0.289 \pm 0.057	0.450 \pm 0.070	0.674 \pm 0.091	0.834 \pm 0.080
image	resnet	max	IUPAC	0.215 \pm 0.070	0.376 \pm 0.110	0.598 \pm 0.170	0.761 \pm 0.188	
image	vit	max	IUPAC	0.215 \pm 0.080	0.365 \pm 0.117	0.575 \pm 0.172	0.740 \pm 0.178	

weaker performance in text generation tasks, further emphasizing the strengths of language models in handling complex linguistic structures and content variability.

Molecular Retrieval. In molecular cross-modal retrieval tasks, the focus is primarily on the retrieval between molecular external information and either internal or external information. We categorize the retrieval tasks into two main types, targeting captions and IUPAC, further subdivided into nine specific retrieval tasks. As shown in Table 5, the IUPAC-to-caption and SMILES-to-IUPAC tasks achieve the best results in their respective categories. Regarding the models, the t5 family demonstrates superiority over bart, encoder-only models, and graph encoders.

Property Prediction. We categorize the tasks into classification and regression, testing them across scaffold and random data splitting methodologies. The evaluation extends to nine distinct datasets, each encompassing three text

Table 6: Experimental Results for Classification Tasks

Task	Data Splitting	Dataset	Input	Encoder	Pooling	roc_auc \uparrow	pr_auc \uparrow	f1_score \uparrow
property prediction (classification)	scaffold	bace	SELFIES	roberta	max	0.742 \pm 0.036	0.750 \pm 0.013	0.544 \pm 0.126
		bace	SELFIES	molt5	max	0.708 \pm 0.065	0.678 \pm 0.043	0.391 \pm 0.033
		bace	InChI	bart	avg	0.704 \pm 0.058	0.699 \pm 0.063	0.516 \pm 0.112
		bace	InChI	t5	max	0.703 \pm 0.030	0.699 \pm 0.043	0.646 \pm 0.032
		bace	InChI	molt5	max	0.678 \pm 0.039	0.699 \pm 0.036	0.565 \pm 0.038
		bbbp	graph	gin	avg	0.652 \pm 0.009	0.684 \pm 0.024	0.528 \pm 0.026
		bbbp	graph	gat	avg	0.651 \pm 0.013	0.691 \pm 0.013	0.470 \pm 0.057
		bbbp	SMILES	molt5	avg	0.651 \pm 0.010	0.692 \pm 0.010	0.602 \pm 0.034
		bbbp	graph	gcn	max	0.645 \pm 0.011	0.693 \pm 0.013	0.492 \pm 0.118
		bbbp	graph	gcn	avg	0.641 \pm 0.012	0.675 \pm 0.014	0.536 \pm 0.057
		clintox	SELFIES	t511	avg	0.923 \pm 0.003	0.722 \pm 0.047	0.483 \pm 0.000
		clintox	InChI	t5	avg	0.908 \pm 0.011	0.700 \pm 0.022	0.483 \pm 0.000
		clintox	SELFIES	t5	avg	0.899 \pm 0.064	0.749 \pm 0.096	0.483 \pm 0.000
		clintox	SELFIES	t5	max	0.874 \pm 0.020	0.721 \pm 0.034	0.381 \pm 0.144
		clintox	InChI	molt5	avg	0.874 \pm 0.039	0.667 \pm 0.039	0.483 \pm 0.000
		sider	SMILES	t511	avg	0.563 \pm 0.029	0.606 \pm 0.006	0.426 \pm 0.026
		sider	graph	gat	avg	0.557 \pm 0.007	0.605 \pm 0.003	0.442 \pm 0.014
		sider	graph	gat	max	0.551 \pm 0.021	0.598 \pm 0.014	0.455 \pm 0.010
		sider	InChI	t5	avg	0.550 \pm 0.016	0.601 \pm 0.014	0.459 \pm 0.011
		sider	graph	gcn	max	0.545 \pm 0.026	0.607 \pm 0.016	0.443 \pm 0.003
		tox21	graph	gin	avg	0.693 \pm 0.019	0.248 \pm 0.037	0.473 \pm 0.000
		tox21	graph	gcn	avg	0.679 \pm 0.007	0.231 \pm 0.007	0.473 \pm 0.000
		tox21	SMILES	molt5	avg	0.664 \pm 0.031	0.200 \pm 0.058	0.488 \pm 0.021
		tox21	graph	gat	avg	0.664 \pm 0.014	0.212 \pm 0.003	0.473 \pm 0.000
		tox21	SMILES	t511	avg	0.657 \pm 0.043	0.212 \pm 0.050	0.486 \pm 0.018
		toxcast	graph	gat	avg	0.606 \pm 0.005	0.305 \pm 0.002	0.449 \pm 0.003
		toxcast	graph	gcn	avg	0.604 \pm 0.006	0.306 \pm 0.002	0.452 \pm 0.003
		toxcast	graph	gin	avg	0.599 \pm 0.008	0.294 \pm 0.016	0.446 \pm 0.001
		toxcast	SMILES	t511	avg	0.582 \pm 0.008	0.302 \pm 0.006	0.451 \pm 0.007
		toxcast	SELFIES	t511	avg	0.579 \pm 0.002	0.293 \pm 0.002	0.453 \pm 0.002
		bace	graph	gcn	avg	0.824 \pm 0.034	0.752 \pm 0.023	0.683 \pm 0.142
		bace	graph	gat	avg	0.782 \pm 0.022	0.715 \pm 0.037	0.398 \pm 0.039
		bace	graph	gin	avg	0.751 \pm 0.034	0.684 \pm 0.061	0.399 \pm 0.042
		bace	SMILES	t5	avg	0.712 \pm 0.043	0.609 \pm 0.056	0.429 \pm 0.089
		bace	InChI	t511	avg	0.710 \pm 0.036	0.656 \pm 0.035	0.459 \pm 0.065
		bbbp	graph	gcn	avg	0.872 \pm 0.014	0.935 \pm 0.017	0.769 \pm 0.031
		bbbp	SMILES	molt5	avg	0.849 \pm 0.062	0.928 \pm 0.036	0.757 \pm 0.071
		bbbp	graph	gat	avg	0.848 \pm 0.020	0.932 \pm 0.013	0.768 \pm 0.012
		bbbp	SMILES	t511	avg	0.848 \pm 0.015	0.940 \pm 0.002	0.742 \pm 0.016
		bbbp	SMILES	t5	avg	0.847 \pm 0.027	0.932 \pm 0.017	0.756 \pm 0.003
		clintox	SMILES	t5	avg	0.861 \pm 0.041	0.654 \pm 0.029	0.485 \pm 0.000
		clintox	SMILES	molt5	avg	0.852 \pm 0.023	0.643 \pm 0.026	0.478 \pm 0.004
		clintox	SELFIES	t5	avg	0.850 \pm 0.004	0.611 \pm 0.027	0.484 \pm 0.003
		clintox	SMILES	t511	avg	0.845 \pm 0.063	0.652 \pm 0.088	0.482 \pm 0.009
		clintox	SELFIES	t511	avg	0.839 \pm 0.022	0.607 \pm 0.009	0.483 \pm 0.005
		sider	SMILES	t5	avg	0.581 \pm 0.031	0.629 \pm 0.015	0.475 \pm 0.017
		sider	graph	gat	max	0.580 \pm 0.018	0.600 \pm 0.002	0.439 \pm 0.013
		sider	InChI	t5	avg	0.568 \pm 0.038	0.618 \pm 0.017	0.461 \pm 0.015
sider	SMILES	molt5	avg	0.562 \pm 0.008	0.600 \pm 0.008	0.461 \pm 0.012		
sider	graph	gin	max	0.561 \pm 0.018	0.618 \pm 0.011	0.451 \pm 0.008		
tox21	graph	gcn	avg	0.795 \pm 0.023	0.283 \pm 0.021	0.481 \pm 0.001		
tox21	graph	gin	avg	0.752 \pm 0.025	0.224 \pm 0.025	0.480 \pm 0.001		
tox21	SMILES	t511	avg	0.745 \pm 0.008	0.246 \pm 0.041	0.494 \pm 0.021		
tox21	SMILES	molt5	avg	0.738 \pm 0.011	0.268 \pm 0.011	0.492 \pm 0.013		
tox21	graph	gin	max	0.733 \pm 0.016	0.214 \pm 0.010	0.480 \pm 0.001		
toxcast	SMILES	molt5	avg	0.673 \pm 0.003	0.336 \pm 0.017	0.465 \pm 0.007		
toxcast	InChI	t5	avg	0.673 \pm 0.018	0.322 \pm 0.027	0.471 \pm 0.001		
toxcast	SELFIES	molt5	avg	0.663 \pm 0.014	0.319 \pm 0.014	0.469 \pm 0.004		
toxcast	graph	gcn	avg	0.662 \pm 0.033	0.325 \pm 0.030	0.464 \pm 0.007		
toxcast	SMILES	t511	avg	0.657 \pm 0.038	0.318 \pm 0.029	0.464 \pm 0.009		

modalities, eight text encoders, and three graph models, integrated with two different pooling strategies. Consequently, each dataset is tested with 108 unique experimental setups. For each combination of input data and model, we select the top five performing models, as shown in Tables 6 and 7.

Table 7: Experimental Results for Regression Tasks

Task	Data Splitting	Dataset	Input	Encoder	Pooling	mse ↓	rmse ↓	mae ↓
property prediction (regression)	scaffold	esol	SMILES	t5	avg	1.573 ± 0.139	1.253 ± 0.056	0.972 ± 0.027
		esol	SMILES	molt5	avg	1.593 ± 0.408	1.252 ± 0.158	0.974 ± 0.102
		esol	InChI	molt5	avg	1.739 ± 0.089	1.318 ± 0.034	0.965 ± 0.038
		esol	graph	gat	avg	1.750 ± 0.173	1.321 ± 0.066	0.983 ± 0.057
		esol	SMILES	t511	avg	1.910 ± 0.533	1.369 ± 0.192	1.039 ± 0.125
		freesolv	graph	gcn	max	9.701 ± 1.892	3.101 ± 0.295	2.254 ± 0.225
		freesolv	SELFIES	molt5	avg	9.858 ± 0.294	3.139 ± 0.047	2.391 ± 0.007
		freesolv	graph	gat	avg	10.429 ± 2.184	3.212 ± 0.332	2.608 ± 0.267
		freesolv	SELFIES	t5	avg	11.689 ± 0.942	3.416 ± 0.140	2.451 ± 0.113
		freesolv	SELFIES	t511	avg	11.740 ± 3.591	3.389 ± 0.504	2.637 ± 0.411
		lipophilicity	graph	gin	avg	0.676 ± 0.067	0.821 ± 0.040	0.656 ± 0.043
		lipophilicity	graph	gcn	avg	0.735 ± 0.006	0.857 ± 0.003	0.684 ± 0.007
		lipophilicity	graph	gcn	max	0.770 ± 0.093	0.876 ± 0.052	0.699 ± 0.046
		lipophilicity	graph	gat	avg	0.855 ± 0.067	0.924 ± 0.036	0.736 ± 0.025
	lipophilicity	SMILES	molt5	max	0.890 ± 0.147	0.940 ± 0.077	0.762 ± 0.064	
	random	esol	InChI	t511	avg	0.967 ± 0.071	0.983 ± 0.036	0.718 ± 0.053
		esol	SMILES	molt5	avg	1.035 ± 0.292	1.007 ± 0.142	0.779 ± 0.130
		esol	SMILES	t511	avg	1.201 ± 0.306	1.087 ± 0.138	0.831 ± 0.126
		esol	InChI	molt5	avg	1.234 ± 0.157	1.109 ± 0.070	0.794 ± 0.037
		esol	graph	gcn	max	1.273 ± 0.316	1.120 ± 0.136	0.841 ± 0.103
		freesolv	graph	gcn	max	5.049 ± 0.493	2.244 ± 0.112	1.733 ± 0.031
		freesolv	graph	gat	max	5.175 ± 1.119	2.261 ± 0.251	1.818 ± 0.226
		freesolv	graph	gat	avg	5.536 ± 0.275	2.352 ± 0.058	1.706 ± 0.059
		freesolv	graph	gcn	avg	6.064 ± 1.485	2.443 ± 0.306	1.829 ± 0.218
		freesolv	InChI	t5	avg	7.343 ± 1.255	2.700 ± 0.232	1.920 ± 0.179
		lipophilicity	graph	gin	avg	0.690 ± 0.099	0.828 ± 0.061	0.650 ± 0.043
		lipophilicity	graph	gat	avg	0.717 ± 0.019	0.846 ± 0.011	0.676 ± 0.008
		lipophilicity	graph	gcn	avg	0.785 ± 0.077	0.885 ± 0.043	0.693 ± 0.045
lipophilicity		graph	gcn	max	0.795 ± 0.132	0.888 ± 0.075	0.704 ± 0.080	
lipophilicity	SMILES	molt5	avg	0.887 ± 0.221	0.934 ± 0.121	0.740 ± 0.100		

The scaffold data splitting method inherently increases the complexity of predictions. Unlike molecular retrieval tasks, where the focus is on embedding tasks with textual targets, leading to a better performance of language models over graph encoders. Here, graph encoders generally outperform language models in most cases.